BNL 28043

CONF-800734--1

LIGHT INDUCED ELECTRON TRANSFER REACTIONS OF METAL COMPLEXES

Norman Sutin and Carol Creutz

Department of Chemistry, Brookhaven National Laboratory, Upton, New York 11973, U.S.A.

Abstract - Properties of the excited states of tris(2,2'-bipyridine) and tris(1,10-phenanthroline) complexes of chromium(III), iron(II), ruthenium(II), osmium(II), rhodium(III), and iridium(III) are described. The electron transfer reactions of the ground and excited states are discussed and interpreted in terms of the driving force for the reaction and the distortions of the excited states relative to the corresponding ground states. General considerations relevant to the conversion of light into chemical energy are presented and progress in the use of polypyridine complexes to effect the light induced decomposition of water into hydrogen and oxygen is reviewed.

INTRODUCTION

In less than a decade the photophysics and photochemistry of polypyridine complexes of transition metals has become one of the most active areas of inorganic chemistry. While tris(2,2'-bipyridine)ruthenium(II) ($Ru(bpy)_3^{2+}$) remains the focus of much of this research, complexes of chromium, osmium, iron, rhodium, iridium, and copper have also received attention. Thus the complexes so far reported to be either luminescent and/or photoactive include metal centers from the first, second, and third transition series and the electron configurations d^3, low-spin d^6, and d^{10}. The properties of the ruthenium(II) and osmium(II) metal-to-ligand charge-transfer excited states have been reviewed (1-3). Papers concerning $Cr(bpy)_3^{3+}$ (4-6), $Fe(bpy)_3^{2+}$ (7), CuL_2^+ (L = 4,9-dimethyl-1,10-phenanthroline = 4,9-$(CH_3)_2$phen) (8), $Ir(bpy)_3^{3+}$ (3,9,10) and $Rh(phen)_3^{3+}$ (11) have appeared recently and the photochemistry of these and other inorganic systems has been extensively reviewed (3). An exhaustive review is beyond the scope of this article. Instead we focus on specific properties of these complexes in their ground and excited states, in particular, excited state deactivation mechanisms, excited state thermodynamic properties, and the intrinsic reactivity of these excited states toward electron transfer reactions. We then consider the factors which limit or promote the efficiency of energy storing electron transfer reactions involving the excited state couples. Finally we discuss the requirements for mediators of the photodecomposition of water and review systems in which some of these requirements have been met.

PROPERTIES OF THE EXCITED STATES

In this first part we survey the photoactive excited states of transition metal complexes of polypyridine ligands, consider the electronic structures of these states, their lifetimes, excited state thermodynamic properties, and their intrinsic reactivity toward electron transfer reactions. Complexes of 2,2'-bipyridine are compared wherever possible.

Photophysical properties. The excited states under discussion along with their electronic configurations, lifetimes, and excited state energies are presented in Table 1. The ground state electronic configurations include low-spin d^6 ($Ru(bpy)_3^{2+}$, $Os(bpy)_3^{2+}$, $Fe(bpy)_3^{2+}$, $Rh(phen)_3^{3+}$, $Ir(bpy)_3^{3+}$), d^3 ($Cr(bpy)_3^{3+}$), and d^{10} (CuL_2^+). With the exception of CuL_2^+ (which is pseudo-tetrahedral) the geometries of the ground state complexes are pseudo-octahedral. The excited states $^*ML_3^{n+}$ result from one-photon excitation of the ground state in the visible or near-ultraviolet regions. The fact that excitation occurs at relatively long wavelengths, ranging from ~ 300 nm for $Rh(phen)_3^{3+}$ (11) to 450-500 nm for CuL_2^+ (18), $Ru(bpy)_3^{2+}$ (1), and $Fe(bpy)_3^{2+}$ (7), to nearly 600 nm for $Os(bpy)_3^{2+}$ (1) accounts, in part, for the interest in these and related materials as sensitizers in solar energy storage systems.

The excited states are of three types: metal-centered ligand-field (M(d-d)) excited states ($^*Cr(bpy)_3^{3+}$ and $^*Fe(bpy)_3^{2+}$), metal-to-ligand charge-transfer (MLCT) excited states ($^*Ru(bpy)_3^{2+}$, $^*Os(bpy)_3^{2+}$), and intraligand ($L(\pi-\pi^*)$) excited states ($^*Rh(phen)_3^{3+}$ and $^*Ir(bpy)_3^{3+}$). The nature of $^*CuL_2^+$ is not known, but it has been postulated to be an MLCT state (8).

DISCLAIMER

TABLE 1. Properties of the excited states of transition metal polypyridine complexes in aqueous solutions at room temperature.[a]

Complex		Excited State	ϕ^{*}[b]	ϕ_{aq}[c]	τ[d] (μs)	S.S.[e] (eV)	E^{*}[f] (eV)
$Cr(bpy)_3^{3+}$	$3d^3$	M(d-d)	0.94	0,0.15	77	0.09	1.7
$Fe(bpy)_3^{2+}$	$3d^6$	M(d-d)	~1.0	$<10^{-2}$	0.008	~1.0	~0.9
$Ru(bpy)_3^{2+}$	$4d^6$	MLCT	1.0	10^{-3}	0.6	$\leqslant$0.2	2.1
$Os(bpy)_3^{2+}$	$5d^6$	MLCT	--	—	0.019	~0.1	1.8
$Rh(phen)_3^{3+}$	$4d^6$	L(π-π^*)	~1.0	—	0.3	<0.5	2.8
$Ir(bpy)_3^{3+}$	$5d^6$	L(π-π^*)	—	—	2.4	~0.1	2.8
CuL_2^{+}	$3d^{10}$	MLCT(?)	—	—	—	—	<2.5

[a] Unless otherwise stated, the data are for aqueous solutions at room temperature and were assembled from ref 1-3. bpy = 2,2'-bipyridine, L = 2,9-dimethyl-1,10-phenanthroline.

[b] Quantum yield for excited state formation: data for $Cr(bpy)_3^{3+}$ from ref 5, for $Fe(bpy)_3^{2+}$ from ref 7, for $Ru(bpy)_3^{2+}$ from ref 12, for $Rh(phen)_3^{3+}$ from ref 11.

[c] Photoaquation quantum yield: for $Cr(bpy)_3^{3+}$ at pH < 4.5 and > 9.0, respectively, from ref 5; for $Fe(bpy)_3^{2+}$ from ref 7; for $Ru(bpy)_3^{2+}$ in 1 M HCl from ref 13.

[d] Lifetime in H_2O (ref 1-3) except for $Rh(phen)_3^{3+}$ (acetonitrile, ref 11) and $Ir(bpy)_3^{3+}$ (methanol, ref 10).

[e] Stokes shifts from refs 14, 15, 26, 17, and 9 for Cr, Ru, Os, Rh, and Ir, respectively. The value given for Fe is not a Stokes shift, as the complex does not emit, but is twice the estimated excited state distortion (7).

[f] Excited state energy; that for $Fe(bpy)_3^{2+}$ was estimated in ref 7. E^{*} for CuL_2^{+} is bracketed by the energy of the band at 450 nm.

As far as is known, these excited states are the lowest excited states possible for each complex. The progression M(d-d), MLCT, L(π-π^*) (and the parallel increase in excited state energy E^{*}) on going from first-transition-series metal centers, to divalent second- and third-transition series d^6 metals, to trivalent second- and third-transition-series d^6 metals is not accidental, but arises as a natural consequence of the increasing ligand-field strength through this sequence. As shown in Fig. 1, the separation of the ligand (bpy or phen) π and π^* orbitals is not strongly perturbed by the nature of the metal center. By contrast, the separation of the nonbonding πd and antibonding dσ^* orbitals (Δ) is sensitive to a number of factors: Δ depends on the charge of the ion and is small for the first transition series (~ 2 eV and ~ 1.5 eV for Cr(III) and Fe(II), respectively) and increases on going to the second and third transition series ($\geqslant$ 2 eV and $\geqslant$ 2.5 eV for Ru(II) and Os(II), and $\geqslant$ 2.5 eV and $\geqslant$ 3 eV for the trivalent ions Rh(III) and Ir(III), respectively) (19). Thus as Δ increases from A to B in Fig. 1 the lowest unoccupied orbital for a d^6 metal center changes from dσ^* (e.g. Fe(II) in A) to Lπ^* (Ru(II) or Os(II) in B). The charge increase on going from Ru(II) or Os(II) to Rh(III) or Ir(III) greatly increases the resistance of the metal to oxidation. Consequently, although d^5 Ir(IV) does exist, the lowest excited states observed for these Rh(III) and Ir(III) complexes arise from promotion of a ligand π (rather than a metal d) electron (9), implying that the πd levels have dropped below the π^* levels in energy as is shown in Fig. 1C. This model, being a crude one-electron description, is not at all exact but has the virtue of simply correlating the behavior of the d^6 (and by simple extensions the d^3 and d^{10}) systems in Table 1. The state diagram in the lower portion of Fig. 1 summarizes the effects of these factors on the ordering of the lowest excited states of $Fe(bpy)_3^{2+}$, $Ru(bpy)_3^{2+}$, and $Os(bpy)_3^{2+}$. While the energy of the MLCT state remains approximately constant through this triad, the M(d-d) excited state energy increases with increasing atomic number. Thus $^{*}Fe(bpy)_3^{2+}$ is an M(d-d) state, but $^{*}Ru(bpy)_3^{2+}$ and $^{*}Os(bpy)_3^{2+}$ are MLCT states.

Apart from their light absorption properties these polypyridine complexes have proved attractive photochemical substrates because of other factors illustrated in Table 1. First, ϕ^{*} the quantum yield for formation of $^{*}M(bpy)_3^{n+}$ (eq 1) is near unity. Furthermore, the excited states are long lived and undergo only slow reaction with solvent. Several deactivation mechanisms tend to destroy these excited states in aqueous solution: these include light emission (eq 2) (fluorescence or phosphorescence), nonradiative decay (eq 3),

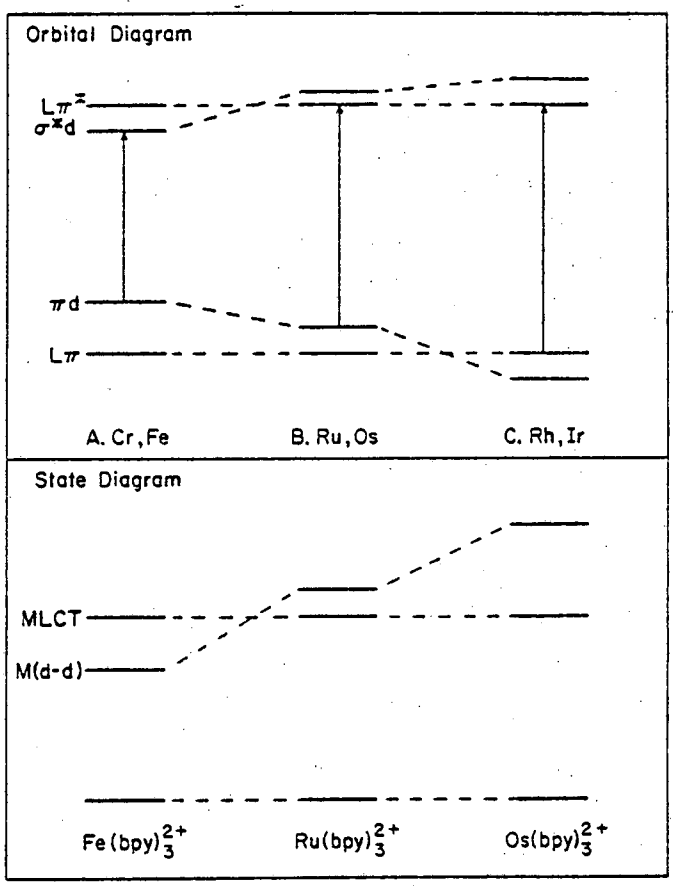

Fig. 1. Orbital and state correlation diagrams for the complexes.

substitution (eq 4), and electron or energy transfer processes involving bimolecular reactions with another solute. The latter are considered in the next section.

$$M(bpy)_3^{n+} \xrightarrow{h\nu} {}^*M(bpy)_3^{n+} \quad (1)$$

$${}^*M(bpy)_3^{n+} \xrightarrow{k_2} M(bpy)_3^{n+} + h\nu' \quad (2)$$

$${}^*M(bpy)_3^{n+} \xrightarrow{k_3} M(bpy)_3^{n+} + \text{heat} \quad (3)$$

$${}^*M(bpy)_3^{n+} + H_2O \xrightarrow{k_4} M(bpy)_2(H_2O)_2^{n+} + bpy \quad (4)$$

or monodentate $M(bpy)_3(H_2O)^{n+}$

The lifetime τ of ${}^*M(bpy)_3^{n+}$ is defined by $1/\tau = (k_2 + k_3 + k_4)$. Values of τ and of $\phi_{aq} = k_4/(k_2 + k_3 + k_4)$ are included in Table 1. For this series, ϕ_{aq} is generally small (the high value for $Cr(bpy)_3^{3+}$ at high pH is atypical). The "photo-inertness" is a consequence, in part, of the fact that bpy and phen, etc., are bidentate ligands and, in part, of the fact that these MLCT and $\pi-\pi^*$ excited states have no greater reactivity toward substitution than the (inert) complexes in their ground states. The M(d-d) $Fe(bpy)_3^{2+}$ excited state is expected to be relatively labile but its lifetime is so short for other reasons that photosubstitution is not a dominant decay pathway. In fact, at room temperature in aqueous solution, nonradiative decay (eq 3) is the dominant excited state deactivation path, i.e. $\tau = 1/k_3$ for all of the complexes listed.

The nonradiative decay of ${}^*M(bpy)_3^{n+}$ to ground state $M(bpy)_3^{n+}$ may be discussed in terms of the thermally equilibrated excited state energy E^* and the differences in nuclear configuration (solvation differences and bond length differences) between ground and excited

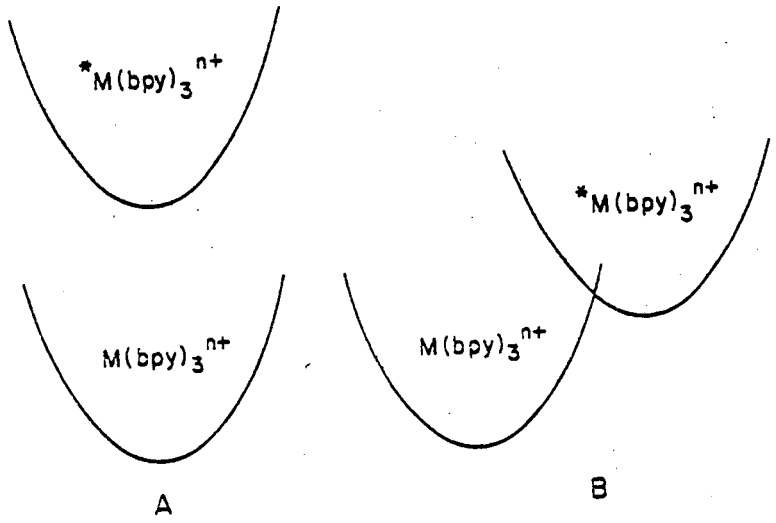

Fig. 2. Relationships between ground- and excited-state potential energy curves: A, small distortion of excited state (small Stokes shift) and B, large excited state distortion.

state complexes (Stokes shift). (See Table 1.) When these differences are small, the potential energy curves for the two states "nestle" as in Fig. 2A. When these differences are large, the ground and excited state curves intersect as in Fig. 2B. In both Fig. 2A and 2B the ground and excited state minima differ in energy by E^*. The difference between the vertical separations of the ground and excited state curves at the minima in the two curves is the Stokes shift (zero in Fig. 2A). With the exception of $Fe(bpy)_3^{2+}$, the $M(bpy)_3^{n+}$ excited states are subject to only small Stokes shifts (Table 1), that is, the nuclear configurations of the MLCT and $L(\pi-\pi^*)$ excited states do not differ much from the nuclear configurations of the d^6 ground states and Fig. 2A is applicable. $Cr(bpy)_3^{3+}$ falls in the same category (6,3) since formation of its ^2E excited state involves no changes in the population of the antibonding σ^*d orbitals. By contrast, the $Fe(bpy)_3^{2+}$ ligand-field state ($(\pi d)^4(\sigma^*d)^2$ or $(\pi d)^5(\sigma^*d)^1$) differs from the d^6 ground state in the population of the σ^*d orbitals and the Fe-N bond distances are likely to be distorted by 0.10-0.16 Å (7). Thus Fig. 2B is relevant for $Fe(bpy)_3^{2+}$. For small Stokes shifts (Fig. 2A) k_3 is determined by Franck-Condon overlap factors between the excited and ground states, the energy gap E^*, and spin-orbit coupling factors. It is not surprising that k_3 is small since the energy gap is relatively large for this series. The surfaces shown in Fig. 2B can be treated in the strong-coupling limit of radiationless transition theory, but they have also been discussed in the language of electron transfer theory (7). Whereas the case depicted in Fig. 2A falls in the inverted region of electron transfer models (and the transition from the upper to the lower surface is slow because of the large driving force E^*), Fig. 2B describes a normal electron transfer whose rate constant decreases with increasing distortion and increases with increasing driving force E^*.

To close this section, we re-emphasize the importance and uniqueness of the photophysical properties of the polypyridine complexes. The ground state molecules have desirable light absorption features. Excitation of the ground state yields $^*M(bpy)_3^{n+}$ in high quantum yield; $^*M(bpy)_3^{n+}$ undergoes little degradation through reaction with solvent. Finally, the fact that $^*M(bpy)_3^{n+}$ lifetimes fall in the microsecond time range means that $^*M(bpy)_3^{n+}$ can undergo bimolecular reactions. This subject is pursued in later sections.

Redox properties. An especially important feature of the polypyridine complexes in Table 1 is that, in the ground state, they may undergo oxidation (eq 5) at the metal center and reduction at the metal or ligand center (eq 6). The ground state potentials $E^o(M^+/M)$ and $E^o(M/M^-)$ defined by eq 5 and 6

$$M(bpy)_3^{(n+1)+} + e^- = M(bpy)_3^{n+} \quad (5)$$

$$M(bpy)_3^{n+} + e^- = M(bpy)_3^{(n-1)+} \quad (6)$$

range from +0.6 to +2.2 V and from -0.3 to -1.3 V, respectively (1,3), and are given in Table 2. Because of their higher energy content E^* (eq 7), the excited states are both stronger reductants (eq 8) and stronger oxidants (eq 9) than the parent ground states.

$$M(bpy)_3^{n+} \longrightarrow {}^*M(bpy)_3^{n+} \qquad E^* \qquad (7)$$

$$M(bpy)_3^{(n+1)+} + e^- = {}^*M(bpy)_3^{n+} \qquad E^o(M^+/{}^*M) \qquad (8)$$

$${}^*M(bpy)_3^{n+} + e^- = M(bpy)_3^{(n-1)+} \qquad E^o({}^*M/M^-) \qquad (9)$$

Redox potentials for the excited couples, calculated (1) from the potentials of the ground-state couples and the excitation energy, are also summarized in Table 2. (It is assumed that the entropy change for eq 7 is small so that E^* may be taken as a free energy.)

TABLE 2. Redox potentials and self-exchange rates for ground and excited state couples.[a]

	Ground State				Excited State			
	M^+/M		M/M^-		$M^+/{}^*M$		${}^*M/M^-$	
Complex	E^o (V)	k ($M^{-1}s^{-1}$)	E^o (V)	k ($M^{-1}s^{-1}$)	E^o (V)	k ($M^{-1}s^{-1}$)	E^o (V)	k ($M^{-1}s^{-1}$)
$Cr(bpy)_3^{3+}$	>1.5	—	-0.26	$\sim 10^9$	>-0.2	—	1.44	$\sim 10^8$
$Fe(bpy)_3^{2+}$	1.05	$\sim 10^9$	-1.26	$\sim 10^8$	$\sim$ 0.1	$< 10^3$	~-0.4	$<10^8$
$Ru(bpy)_3^{2+}$	1.26	$\sim 10^9$	-1.28	$\sim 10^8$	-0.84	$\sim 10^8$	0.83	$\sim 10^8$
$Os(bpy)_3^{2+}$	0.82	$\sim 10^9$	-1.22	$\sim 10^8$	-0.96	$\sim 10^8$	0.67	$\sim 10^8$
$Rh(phen)_3^{3+}$	>1.5	$\sim 10^9$	-0.7	$\sim 10^8$	>-1.3	$< 10^8$	2.00	$< 10^8$
$Ir(bpy)_3^{3+}$	2.17	$\sim 10^9$	-0.76	—	-0.64	$< 10^8$	2.05	$< 10^8$
CuL_2^+	0.63	$\sim 10^4$	—	—	>-1.9	—	—	—

[a] For aqueous solutions, 25°C, E^o's relative to N.H.E. Data from ref 1,3,7 ($Fe(bpy)_3^{2+}$), 11 ($Rh(phen)_3^{3+}$), 8 and 20 (CuL_2^+, L = 2,9-$(CH_3)_2$phen), and ref cited therein.

The intrinsic kinetic barriers to electron transfer processes are reflected in rate constants for electron exchange, eq 10 and 11 for the ground state couples and eq 12 and 13 for the excited state couples. The self exchange rates estimated for these couples are

$$M(bpy)_3^{n+} + M(bpy)_3^{(n+1)+} \rightleftharpoons M(bpy)_3^{(n+1)+} + M(bpy)_3^{n+} \qquad (10)$$

$$M(bpy)_3^{(n-1)+} + M(bpy)_3^{n+} \rightleftharpoons M(bpy)_3^{n+} + M(bpy)_3^{(n-1)+} \qquad (11)$$

$${}^*M(bpy)_3^{n+} + M(bpy)_3^{(n+1)+} \rightleftharpoons M(bpy)_3^{(n+1)+} + {}^*M(bpy)_3^{n+} \qquad (12)$$

$$M(bpy)_3^{(n-1)+} + {}^*M(bpy)_3^{n+} \rightleftharpoons {}^*M(bpy)_3^{n+} + M(bpy)_3^{(n-1)+} \qquad (13)$$

included in Table 2. The high self-exchange rates of the ruthenium(II) and osmium(II) MLCT couples has been previously noted (1). The d^5 metal center in ${}^*M(bpy)_3^{2+}$ (M = Ru or Os) should resemble that in $M(bpy)_3^{3+}$ while the $L\pi^*$ region in ${}^*M(bpy)_3^{2+}$ provides a model for $M(bpy)_3^+$ which has the electronic configuration $(d)^6(\pi^*)^1$. The small Stokes shift for ${}^*M(bpy)_3^{2+}/M(bpy)_3^{2+}$ requires that solvation and metal-ligand and intraligand bond lengths differ very little between $M(bpy)_3^{2+}$ and ${}^*M(bpy)_3^{2+}$ and, by analogy, between ${}^*M(bpy)_3^{2+}$, $M(bpy)_3^{3+}$, and $M(bpy)_3^+$, as well. This expectation is borne out by the exchange rates of the ground and excited state couples (10^8-10^9 M^{-1} s^{-1}) which are near the diffusion-controlled limit. Since the reorganizational requirements will be small for other low-spin d^5/d^6 couples (Fe(III)/Fe(II), Rh(IV)/Rh(III) and Ir(IV)/Ir(III) ground state species) these exchange rates will also be very large. Furthermore, other exchange processes involving transfer of a π^* electron to an empty π^* orbital (for example, ground state $Fe(bpy)_3^{2+}/Fe(bpy)_3^+$) should also be very rapid. No information concerning the CuL_2^+ excited state couples nor the d^2/d^3 ground and excited state $Cr(bpy)_3^{4+}/Cr(bpy)_3^{3+}$ couples and their self-exchange rates is at present available. Both ground and excited (^2E) $Cr(bpy)_3^{3+}/Cr(bpy)_3^{2+}$ couples involve $(\pi d)^3/(\pi d)^4$ electronic configurations. The ground

state self-exchange rate is very rapid as is the excited state process. This is expected from the fact that changing the electron population of the πd levels in polypyridine complexes results in only negligible reorganization barriers (1). The relationship between excited state exchange rates and Stokes shifts has been discussed elsewhere (3,6).

By contrast to the above systems, because of the presence of σ*d electrons $^*Fe(bpy)_3^{2+}$ (M(d-d), either $(\pi d)^5(\sigma^* d)^1$ or $(\pi d)^4(\sigma^* d)^2$) is considerably distorted with respect to $Fe(bpy)_3^{2+}$, $Fe(bpy)_3^{3+}$, and $Fe(bpy)_3^{+}$ (7). As a consequence the exchange reactions of this excited state possess a substantial activation barrier. In addition, if the M(d-d) state has the electronic configuration $(\pi d)^4(\sigma^* d)^2$, the probability of electron transfer (adiabaticity) is diminished since there is no correlation of the reactants and products of the one-electron transfer process; i.e., the processes

$$\underset{(\pi d)^4(\sigma^* d)^2}{{}^*Fe(bpy)_3^{2+}} + \underset{(\pi d)^5}{Fe(bpy)_3^{3+}} \longrightarrow \underset{(\pi d)^5}{Fe(bpy)_3^{3+}} + \underset{(\pi d)^4(\sigma^* d)^2}{{}^*Fe(bpy)_3^{2+}}$$

and

$$\underset{(\pi d)^4(\sigma^* d)^2}{{}^*Fe(bpy)_3^{2+}} + \underset{(\pi d)^6(L\pi^*)^1}{Fe(bpy)_3^{+}} \longrightarrow \underset{(\pi d)^6(L\pi^*)^1}{Fe(bpy)_3^{+}} + \underset{(\pi d)^4(\sigma^* d)^2}{{}^*Fe(bpy)_3^{2+}}$$

cannot be accomplished through a simple one-electron change. Similar constraints on the electron transfer probability apply as well for the $L(\pi-\pi^*)$ excited states of $Rh(phen)_3^{3+}$ and $Ir(bpy)_3^{3+}$ if $Rh(phen)_3^{2+}$ and $Ir(bpy)_3^{2+}$ are $(\pi d)^6(\sigma^* d)^1$ and $Rh(phen)_3^{4+}$ and $Ir(bpy)_3^{4+}$ are $(\pi d)^5$. Thus the electron exchange rate constants for all four of these couples should be much less than those for the ruthenium and osmium complexes, that is, $\ll 10^8\ M^{-1}\ s^{-1}$.

In Table 1, the excited states of highest energy content are the $Rh(phen)_3^{3+}$ and $Ir(bpy)_3^{3+}$ $L(\pi-\pi^*)$ states. Both have reasonably long lifetimes so that scavenging of these species in bimolecular reactions with other solute molecules is feasible. Furthermore, both are very strong reductants (eq 7) and oxidants (eq 8) (Table 2). Despite the fact that their ground states have only poor visible-light absorption characteristics, these systems merit much greater study. By contrast, the M(d-d) state of $Fe(bpy)_3^{2+}$ has only low excitation energy, is a relatively poor oxidant and reductant, manifests a low inherent transfer reactivity, and has a very short lifetime. Therefore, despite its high visible absorptivity, $Fe(bpy)_3^{2+}$ is unlikely to prove of any great value in solar energy conversion schemes. No conclusions concerning the possible utility of $^*CuL_2^{+}$ can be drawn at present since so few data are available. The M(d-d) state $^*Cr(bpy)_3^{3+}$ is a very strong oxidant, producing the relatively good reductant $Cr(bpy)_3^{2+}$ upon reduction. While $Cr(bpy)_3^{3+}$ shows only modest visible-light absorption, the 77 μs lifetime of the excited state is extremely useful. The highly colored $Ru(bpy)_3^{2+}$ and $Os(bpy)_3^{2+}$ complexes both have strongly reducing and modestly oxidizing excited states, but the excited ruthenium complex offers advantages over the excited osmium complex because of its much longer lifetime. Both $^*Ru(bpy)_3^{2+}$ and $^*Cr(bpy)_3^{3+}$ have high electron exchange rates and a number of their electron transfer reactions have been characterized. Because of their desirable properties and because a useful body of information concerning their reactivity now exists, $^*Ru(bpy)_3^{2+}$ and $^*Cr(bpy)_3^{3+}$ are likely to prove particularly useful in solar energy conversion schemes.

PHOTOINDUCED ELECTRON TRANSFER

If the excited state of a molecule (sensitizer, S) is sufficiently long lived it may undergo bimolecular reaction with another solute molecule (quencher, Q). The three bimolecular processes most frequently encountered involve electron transfer from the excited state to an acceptor (eq 14, oxidative quenching), electron transfer from a donor to the excited state (eq 15, reductive quenching), and energy transfer from the excited molecule to a ground state quencher to form the excited state quencher (eq 16). The latter process is discussed

$$^*S + Q \xrightarrow{k_q} S^+ + Q^- \qquad (14)$$

$$^*S + Q \xrightarrow{k_q} S^- + Q^+ \qquad (15)$$

$$^*S + Q \xrightarrow{k_q} S + {}^*Q \qquad (16)$$

in detail elsewhere (3,6,7). The electron transfer processes eq 14 and 15 are generally followed by back reactions to form ground state reactants (eq 17 and 18).

$$S^+ + Q^- \xrightarrow{k_t} S + Q \qquad (17)$$

$$S^- + Q^+ \xrightarrow{k_t} S + Q \qquad (18)$$

Light absorption by a ground state molecule yields an excited state in which light energy is stored (if only briefly) as chemical energy. The length of time for which the energy is stored may be increased through electron transfer quenching, since the reaction of the excited state with an electron acceptor or donor may give high energy electron transfer products. If the separated products can be preserved or converted into other useful products, storage of some of the original excitation energy can be accomplished. Unfortunately the fact that high energy products are obtained in the quenching steps above implies that unproductive back reaction between them (eq 17,18) is likely to be very rapid. Clearly, efficient use of excited state electron transfer reactions for energy storage requires efficient excited state quenching (large k_q), but slow back reaction rates (small k_t). Theoretical models provide some guidelines as to how this may be accomplished.

General considerations. We first consider that the quenching and back reactions are not coupled; this treatment is appropriate provided that the rate of the back reaction does not approach the diffusion-controlled limit. Under these conditions the quenching and back reactions each proceed in three steps as shown in Scheme I (21).

Scheme I

$$^*S + Q \rightleftharpoons {}^*S|Q \qquad K_o$$

$$^*S|Q \longrightarrow S^+|Q^- \qquad k_{e\ell}$$

$$S^+|Q^- \longrightarrow S^+ + Q^-$$

The first step is the formation of a precursor complex from the separated reactants. Electron transfer within the precursor complex to form the successor complex occurs in the second step. The successor complex dissociates into separated products in the third step. If the reaction is not diffusion controlled, the observed rate constant is equal to $K_o k_{e\ell}$, where K_o is the equilibrium constant for the formation of the precursor complex and $k_{e\ell}$ is the (first-order) rate constant for electron transfer within the precursor complex. In general, a number of precursor complexes, each characterized by a different separation of the reactants, reactant orientation, "intramolecular" electron transfer rate, etc., may be present.

The value of K_o depends upon the electrostatic and non-electrostatic interactions of the reactants with one another and with the medium. The magnitude of these interactions is determined by such factors as the charges on the reactants, their sizes, their hydrophilic or hydrophobic character, the dielectric constant of the medium, etc. Steric and orientation factors are also included in K_o. The rate constant $k_{e\ell}$ is given by

$$k_{e\ell} = \kappa \frac{kT}{h} \exp\left\{-\frac{\Delta G^*}{RT}\right\}$$

where κ is the electronic transmission coefficient and ΔG^* is the energy required to reorganize the reactants and the surrounding medium prior to the electron transfer. The value of κ depends upon the electronic coupling of the two reactants; it is unity for an adiabatic reaction and less than unity for a nonadiabatic reaction (22). ΔG^* is determined by the difference in the nuclear configurations of the reactants and products (the smaller this difference, the more rapid the electron transfer), the sizes and separation of the reactants, the dielectric constant and refractive index of the medium, and the standard free energy change for the electron transfer (23,24) (for an exchange reaction, ΔG° is equal to zero and thus ΔG^* for the exchange reaction is equal to the intrinsic electron transfer barrier for the couple).

Although the quenching and back reactions have been treated separately, back reaction of the primary products of the quenching reaction can occur before they have diffused out of the cage in which they were formed. This is allowed for in Scheme II.

Scheme II

$$^*S + Q \underset{k_{21}}{\overset{k_{12}}{\rightleftharpoons}} {}^*S|Q \underset{k_{32}}{\overset{k_{23}}{\rightleftharpoons}} S^+|Q^- \underset{k_{43}}{\overset{k_{34}}{\rightleftharpoons}} S^+ + Q^-$$

$$^*S \xrightarrow{h\nu} S + Q \rightleftharpoons S|Q \qquad S^+|Q^- \xrightarrow{k_{30}} S|Q$$

If k_{32} is neglected, the yield of the primary electron transfer products S^+ and Q^- is equal to $k_{34}/(k_{30} + k_{34})$. Since k_{30} is a rate constant for electron transfer within a precursor complex, its value is determined by the same factors that determine the value of $k_{e\ell}$. On the other hand, k_{34} is the rate constant for the diffusion of the products from the cage in which they were formed and its value depends on the diffusion coefficients of S^+ and Q^- and on the same factors that determine the value of K_o.

Examples of the way in which the reorganization energy of the couples and the driving force affect $k_{e\ell}$ are given in Fig. 3.

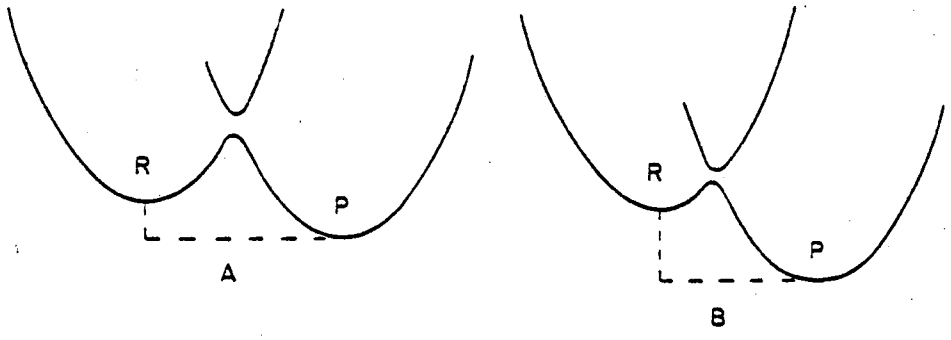

Fig. 3. Plot of potential energy versus nuclear configuration. For (A) the couples have high intrinsic barriers to electron transfer and the driving force for the reaction is small; for (B) the intrinsic barriers are small and the driving force is large.

The magnitude of the reorganization energies (self-exchange rates) of the couples is reflected in the horizontal distance between the minima of the reactant and product potential-energy curves, while the magnitude of the driving force for the electron transfer is reflected in the vertical distance between the minima. The activation barrier is relatively large for reactions involving couples with large reorganization energies and small driving forces (Fig. 3A), while the activation barrier is relatively small for reactions involving couples with small reorganization energies and large driving forces (Fig. 3B). Thus, because of the larger reorganization energy (slower self-exchange rate, Table 2) of the $^*Fe(bpy)_3^{2+}$ couples, reactions of $^*Fe(bpy)_3^{2+}$ are expected to be much slower than those of the other bipyridine and phenanthroline complexes included in Table 2. In addition, the driving force for $^*Fe(bpy)_3^{2+}$ reactions is also relatively small so that Fig. 3A is applicable. By contrast, analogous reactions of $^*Ru(bpy)_3^{2+}$ involve smaller intrinsic barriers and greater driving force (Fig. 3B). As will be seen, this prediction is borne out by the data.

Provided that the driving force is not too large, the electron transfer rate should increase with increasing driving force (the normal region) until the reaction is diffusion controlled. Increasing the driving force still further should then decrease the electron transfer rate (the inverted region) (23,25). This is shown in Fig. 4, a plot of potential energy as a function of nuclear configuration, for electron transfer in the normal (A) and inverted (B) regions.

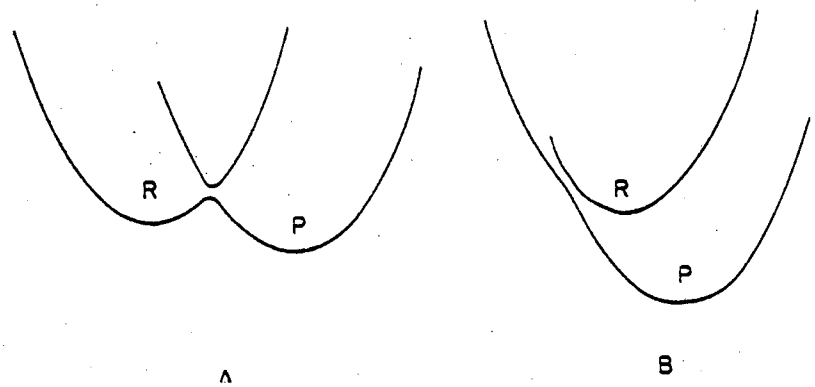

Fig. 4. Plot of potential energy versus nuclear configuration for electron transfer in (A), the normal, and (B), the inverted region.

There is considerable evidence for the increase in quenching rate constant with driving force below the diffusion-controlled limit (1-3,6,32,36). The rate constant for the quenching reaction can thus be increased in the normal free-energy region by increasing its driving force. Since $E^* = (\Delta G_q^\circ + \Delta G_t^\circ)$, increasing the driving force for the quenching reaction will simultaneously decrease the driving force for the back reaction, thereby decreasing its rate. Unfortunately increasing the driving force for the quenching reaction will decrease the fraction of the excitation energy available for storage. The inverted region offers a way out of this dilemma: since rates increase with decreasing driving force in the inverted region it is possible to simultaneously obtain rapid quenching, slow back reaction, and efficient energy storage. Although nuclear tunneling effects will diminish the rate decreases in the inverted region, they will not eliminate it entirely (25) (cf. the energy gap law of radiationless transition theory) and rather large rate decreases in the inverted region have recently been reported (26). The finite cage escape yields found for some very exothermic back reactions could have their origins in the rate decreases inherent in the inverted region.

In general, the factors determining electron transfer rates cannot be varied independently for the quenching and back reactions. Thus the charges on the reactants and products are, of course, related (but can be chosen to favor the quenching reaction and to slow down the back reaction). Similarly, the free energy changes for the quenching and back reactions are also related, their sum being equal in magnitude to the excitation energy. On the other hand, the electronic coupling of the reactants in the quenching and back reactions are not necessarily related since different orbitals are involved in the two reactions. For example, the oxidative quenching of $^*RuL_3^{2+}$ involves the transfer of an electron from a ligand π^* orbital to a suitable acceptor, while the back reaction involves the transfer of an electron from the reduced acceptor to the πd orbitals of the ruthenium center. In certain instances the quenching and back reactions may also be subject to different spin multiplicity restrictions. The net effect is that under certain conditions the quenching reaction may be adiabatic and the back reaction, nonadiabatic. Because of nonadiabatic effects, electron transfer rates may limit below the diffusion-controlled rate, even at very large driving force (22). Thus nonadiabaticity could also be responsible for the finite cage escape yields of very exothermic back reactions. These and other factors are now illustrated for specific systems.

Quenching reactions. Quenching of $^*Ru(bpy)_3^{2+}$ by $Rh(bpy)_3^{3+}$ proceeds with a rate constant k_q of 6.2×10^8 M^{-1} s^{-1} in 0.5 M H_2SO_4 at 25°C (27-29) and flash photolysis studies have shown that $Ru(bpy)_3^{3+}$ and $Rh(bpy)_3^{2+}$ are produced (28). Thus oxidative quenching of $^*Ru(bpy)_3^{2+}$ (eq 14) by $Rh(bpy)_3^{3+}$ is implicated. The dependence of the quenching rate on the potentials of the couples is illustrated by recent studies with the derivatives of these ruthenium and rhodium complexes, RuL_3^{2+} and RhL_3^{3+}. Quenching rate constants measured (29,30) for eq 19 and 20 range from 3×10^7 to 1.7×10^9 M^{-1} s^{-1}. These rate variations

$$^*RuL_3^{2+} + Rh(bpy)_3^{3+} \longrightarrow RuL_3^{3+} + Rh(bpy)_3^{2+} \qquad (19)$$

$$^*Ru(bpy)_3^{2+} + RhL_3^{3+} \longrightarrow Ru(bpy)_3^{3+} + RhL_3^{2+} \qquad (20)$$

reflect the changing driving force for electron transfer from the excited ruthenium complex to the ground state rhodium(III) complex as the polypyridine ligands are varied; $E^\circ(M^+/^*M)$ for RuL_3^{2+} varies from -0.77 V (L = 5-chloro-1,10-phenanthroline) to -1.01 V (L = 4,7-dimethyl-1,10-phenanthroline (1) and the potentials of the RhL_3^{3+}/RhL_3^{2+} couples encompass a similar range (30). Thus the equilibrium constant for eq 19,20 may be varied over a factor of more than 10^4. For this series log k_q increases with increasing ΔE° until k_q values around 10^9 M^{-1} s^{-1} are attained. As is expected from Scheme II, this leveling occurs because diffusion together of the reactants ($k_{12} \sim 3 \times 10^9$ M^{-1} s^{-1} for reactions of this type), rather than electron transfer (k_{23}) is becoming rate limiting. Similar linear free energy relationships (in the region below the diffusion limit) have been obtained for the reductive quenching of $^*CrL_3^{3+}$ by Fe_{aq}^{2+} (6); k_q ranges from (0.1-5) $\times 10^7$ M^{-1} s^{-1} over a ΔE° span of 0.4 V.

A cross-section of rate constants obtained for both oxidative and reductive quenching of $^*Ru(bpy)_3^{2+}$ is presented in Table 3. The driving force for oxidative quenching by Eu_{aq}^{3+} and MV^{2+} (methylviologen, MV^{2+} = N,N'-dimethyl-4,4'-bipyridinium cation) is similar but the rate constant for quenching by MV^{2+} is ten thousand times greater than for quenching by Eu_{aq}^{3+}. These rate differences reflect the varying reorganization barriers of the oxidant (quencher) couples and, for Eu_{aq}^{3+}, some nonadiabaticity. It is noteworthy that most of the k_q values in Table 3 exceed 10^7 M^{-1} s^{-1}. This is as much a consequence of the 0.6 μs lifetime of this excited state as of its high self-exchange rate. Prohibitively high concentrations (> 1 M) of quenchers which quench more slowly would be required to determine k_q values below 10^6 M^{-1} s^{-1} for $^*Ru(bpy)_3^{2+}$. Much slower quenching ($k_q < 10^5$ M^{-1} s^{-1}) may be obtained with the 77 μs excited state of $Cr(bpy)_3^{3+}$.

Differences in excited state reactivity are dramatically illustrated by the oxidative quenching of $^*Fe(bpy)_3^{2+}$ and $^*Ru(bpy)_3^{2+}$ by Fe_{aq}^{3+} for which k_q is $< 10^7$ M^{-1} s^{-1} (7) and $> 10^9$ M^{-1} s^{-1} (Table 3), respectively. In contrast to the Eu_{aq}^{3+} and MV2+ oxidations of

TABLE 3. Quenching (k_q) and back reaction (k_t) rate constants and cage escape yields (ϕ_{cage}) for reactions of $^*Ru(bpy)_3^{2+}$.[a]

Quencher	k_q (M^{-1} s^{-1})	ΔE_q° (V)	k_t (M^{-1} s^{-1})	ΔE_t° (V)	ϕ_{cage}	Ref.
		Oxidative Quenching of $^*Ru(bpy)_3^{2+}$				
$Rh(bpy)_3^{3+}$	6.2×10^8	0.1	$\sim 3 \times 10^9$	~2	0.15	27-29
$Cr(bpy)_3^{3+}$	3.3×10^9	0.6	2.6×10^9	1.5	> 0	31
MV^{2+}	1.4×10^9	0.37	4×10^9	1.7	0.25	29
Eu_{aq}^{3+}	$\leqslant 0.8 \times 10^5$	0.41	$\sim 3 \times 10^9$	1.7	> 0	32
Fe_{aq}^{3+}	2.7×10^9	1.5	5×10^6	0.6	1.0	32,12
Cu_{aq}^{2+}	6.2×10^7	1.0	9.7×10^8	1.4	0.56	36
		Reductive Quenching of $^*Ru(bpy)_3^{2+}$				
Eu_{aq}^{2+}	2.8×10^7	1.3	4.5×10^7	0.8	1.0	33
ascorbate	2.0×10^7	~0.0	1×10^9	~2.1	~0.5	34,35

[a] Aqueous solutions, $\mu \sim 0.5$ M, 25°C.

$^*Ru(bpy)_3^{2+}$ where the rate differences are ascribed mainly to different intrinsic electron transfer barriers in the one (quenching) couple, these rate differences are due both to intrinsic electron transfer reactivity differences and to differences in driving force for the excited state couples. $^*Fe(bpy)_3^{2+}$, an M(d-d) state, undergoes a substantial rearrangement upon oxidation to $Fe(bpy)_3^{3+}$; $^*Ru(bpy)_3^{2+}$ undergoes little distortion upon oxidation. Furthermore, the driving force for Fe_{aq}^{3+} oxidation of $^*Ru(bpy)_3^{2+}$ exceeds that for oxidation of $^*Fe(bpy)_3^{2+}$ by $\geqslant 0.9$eV (7). Similar considerations apply to the reduction of $^*Fe(bpy)_3^{2+}$ versus that of $^*Ru(bpy)_3^{2+}$. Thus, as discussed earlier, because of its high intrinsic electron-transfer barriers and its relatively low energy content (and short lifetime), $^*Fe(bpy)_3^{2+}$ is unlikely to prove of great value in systems requiring rapid quenching.

Back reactions. In flash-photolysis experiments the relatively rapid reaction of the excited state and quencher to give electron transfer products is followed by the slow restoration of the absorbance of the original ground state species. For $Ru(bpy)_3^{2+}$, $Rh(bpy)_3^{3+}$ solutions the absorbance of ground state $Ru(bpy)_3^{2+}$ is restored on the millisecond time scale with k_t, the rate constant for thermal back reaction of $Rh(bpy)_3^{2+}$ and $Ru(bpy)_3^{3+}$ (eq 21), $\sim 3 \times 10^9$ M^{-1} s^{-1} (28). It is not surprising that this reaction is

$$Ru(bpy)_3^{3+} + Rh(bpy)_3^{2+} \longrightarrow Ru(bpy)_3^{2+} + Rh(bpy)_3^{3+} \qquad (21)$$

so rapid since its driving force is nearly 2V (the quenching reaction is exergonic by only ~ 0.1 V). What is remarkable is that any $Ru(bpy)_3^{3+}$ and $Rh(bpy)_3^{2+}$ escape the quenching products' solvent cage (see Scheme II); the observed cage escape yield is 0.15 ± 0.03. This relatively large cage escape yield may be related to nonadiabaticity and/or to the fact that this back reaction is in the inverted region.

Back reaction (eq 17,18) rate constants and cage escape yields for a number of other systems are included in Table 3. In general, k_t increases and ϕ_{cage} decreases as ΔE_t° for the back reaction increases, although it is evident that the individual Q/Q^+ and Q/Q^- properties also play an important role. The connection between k_t and ϕ_{cage} implicit in Scheme II is supported by observations on the quenching of $^*RuL_3^{2+}$ by Cu_{aq}^{2+} (36). In this series ϕ_{cage} varies from 0.3 to 1.0 as k_t decreases from 2.3×10^9 to 1×10^8 M^{-1} s^{-1} as is expected from eq 22

$$\phi_{cage} = k_{34}/(k_{30} + k_{34}) = (1 - k_t/k_{diff}) \qquad (22)$$

where k_{diff} is the diffusion-controlled limit for the back reaction.

Electrostatic and hydrophobic factors. In the systems we have reviewed so far, we have interpreted rate differences as variations in k_{el}, the electron transfer rate constant, although K_o, which reflects the work required to bring the oxidant and reductant together,

has varied to some extent as well. In fact it is likely that variations in K_o are partly responsible for the great differences seen in both k_q and k_t for reactions of Eu_{aq}^{3+} and MV^{2+} (Table 3). MV^{2+}, MV^{+}, $^*Ru(bpy)_3^{2+}$, and $Ru(bpy)_3^{3+}$ are hydrophobic, while Eu_{aq}^{3+} and Eu_{aq}^{2+} are hydrophilic. Similar considerations apply in the Fe_{aq}^{3+} quenching and Fe_{aq}^{2+} back reactions (Table 3). Non-electrostatic (hydrophobic) factors have previously been invoked to rationalize the relatively slow electron transfer rates measured when one reactant is hydrophilic (e.g. $Fe(CN)_6^{4-}$) and the other is hydrophobic (e.g. $Co(phen)_3^{3+}$) (37,38).

The electrostatic and non-electrostatic interactions of the reactants with one another and the medium can also be considerably modified by the addition of micelles (39) as is shown in Table 4.

TABLE 4. Rate constants for quenching and back reactions of substituted RuL_3^{2+} and viologen derivatives at 25°C.[a]

Complex	R_1, R_2	Conditions	10^{-9} k_q (M^{-1} s^{-1})	10^{-9} k_t (M^{-1} s^{-1})	Ref.
$Ru(bpy)_3^{2+}$	CH_3, CH_3	0.17 M sulfate	1.4	4	29
$Ru(bpy)_3^{2+}$	CH_3, n-$C_{14}H_{29}$	0.0014 M chloride	0.8	4	41
$Ru(bpy)_3^{2+}$	CH_3, n-$C_{14}H_{29}$	0.004-0.02 M CTAC	~0.8	< 0.02	41
$(bpy)_2Ru(bpy(R_3)_2)^{2+}$	n-$C_{12}H_{25}$, n-$C_{12}H_{25}$	0.01 M CTAC	10	0.0002	42,43
$Ru(bpy)_3^{2+}$	CH_3, CH_3	nonaqueous[b]	2.8	8.1	46
$Ru(bpy(COOCH(CH_3)_2)_2)_3^{2+}$	CH_3, CH_3	nonaqueous[b]	0.12	1.8	46
$Ru(bpy(COODHC)_2)_3^{2+}$	CH_3, CH_3	nonaqueous[b]	0.02	1.3	46

[a] R_1 and R_2 are the substituents in N,N'-R_1,R_2-4,4'-bipyridinium cation. DHC is dihydrocholesterol; CTAC is cetyltrimethylammonium chloride; R_3 is (-$CONHC_{12}H_{25}$).
[b] The medium is 1:1 acetonitrile:isobutyronitrile containing 0.1 M tetraethylammonium hexafluorophosphate.

The negatively-charged micelle sodium dodecyl sulfate (SDS) decreases the rate of the reaction of $Ru(bpy)_3^{3+}$ with $Fe(CN)_6^{4-}$ by two to three orders of magnitude (40). Similarly, the positively-charged micelle cetyltrimethylammonium chloride (CTAC) markedly decreases the rate constant for $C_{14}MV^{2+}$ (8×10^8 M^{-1} s^{-1}) is hardly altered, but the $C_{14}MV^{+}$ produced in the quenching is rapidly bound by the micelle and the back reaction rate constant is decreased from 4×10^9 to $< 2 \times 10^7$ M^{-1} s^{-1} (41). Similar effects of CTAC on the back reaction following the reductive quenching of the hydrophobic $(bpy)_2Ru(bpy(CONHC_{12}H_{25})_2)^{2+}$ derivative by dimethylaniline (DMA) have been reported (42-44): the back reaction rate constant is 7.8×10^9 M^{-1} s^{-1} in acetonitrile, but only 2.6×10^7 M^{-1} s^{-1} in 0.01 M aqueous CTAC. As expected, the CTAC dramatically decreases the rate for quenching of the ruthenium derivative by MV^{2+} ($k_q = 2 \times 10^5$ M^{-1} s^{-1}) but not by $(C_{12})_2V^{2+}$, a hydrophobic MV^{2+} derivative in which both methyl groups have been replaced by n-dodecyl groups (42-44).

Although it is difficult to analyze the above effects quantitatively since they involve changes in concentration, reactant distances, medium (and local) dielectric constants, electrostatic potentials, driving force, etc., it is clear that very large changes in overall electron transfer rates can be produced by the addition of micelles (45). An important point that remains to be established in some cases, for example, the $C_{14}MV^{2+}$ system described above, is whether in addition to slowing down the back reaction the micelle also increases the cage escape yield of the primary quenching products.

Some of the effects produced by micelles may have their origin in changes in the steric and nonadiabatic factors. Evidence for the operation of such factors in the absence of micelles is provided by the reactions of a series of $Ru(bpy(COOR)_2)_3^{2+}$ complexes in organic solvents (46-48). The rate constants for oxidation of these excited states by MV^{2+} are twenty to two-hundred times slower than those for oxidation by $^*Ru(bpy)_3^{2+}$. Perhaps more importantly, the back reactions are also slowed down, but to a smaller extent. The largest effect is seen when R = dihydrocholestrol (Table 4). These effects arise in part from changes in the driving force for the electron transfer; when this is taken into account the magnitudes of the quenching rate constant decreases are diminished, but the quenching of the dihydrocholesterol ester still proceeds about forty times more slowly than the quenching of

$Ru(bpy)_3^{2+}$. This remaining decrease presumably reflects changes in the sizes of the reactants and in the local dielectric constant, in addition to changes in the steric and electronic overlap factors. Consistent with the above observations, relatively large back reaction rate decreases are obtained with reductive quenchers; indeed when R = isopropyl and the quencher is Et_3N the back reaction rate is sufficiently slow for the Et_3N^+ produced in the quenching reaction to abstract an H atom from Et_3N, allowing the accumulation of RuL_3^+ in the solution (47).

To conclude, in the normal course of events the quenching reaction is followed by a back reaction that returns the system to its original composition. The net effect of the excitation, quenching, back reaction sequence is that the light energy which is temporarily stored as chemical energy through the quenching reaction, is converted into heat. Another way of looking at this sequence is that the absorption of light produces an electron-hole pair in the excited molecule (eq 23); this electron-hole pair, normally recombines through radiative and radiationless decay processes (eq 24).

$$S \xrightarrow{h\nu} {}^+S^- \qquad (23)$$

$$ {}^+S^- \longrightarrow S \qquad (24)$$

The quenching reactions compete with these physical deactivation processes. Through the quenching reactions (shown here for oxidative quenching) the electron and hole become localized on different molecules (eq 25), and ultimately recombine through the back reaction (eq 26). Equations 25 and 26 are thus analogous to eq 23 and 24, with the quencher

$$ {}^+S^- + Q \longrightarrow S^+ + Q^- \qquad (25)$$

$$S^+ + Q^- \longrightarrow S + Q \qquad (26)$$

extending the electron-hole separation initiated by the photon and the back reaction fulfilling the role of radiative and nonradiative processes which deactivate the original excited state. In this section we have seen that $k_{e\ell}$ for both quenching and back reactions is a function of driving force, intrinsic electron transfer barriers, and the nonadiabaticity of the electron transfer reaction whether ground or excited state processes are involved. Furthermore, we have seen how manipulation of K_o through introduction of hydrophobic substituents and the addition of micelles to the medium may alter both quenching and back reaction rates. In the next section we describe systems in which further chemical processes compete with the back reaction so that net conversion of light energy into chemical energy does occur. In particular, we consider systems in which the quenching reaction is coupled to oxidation-reduction reactions that ultimately yield hydrogen or oxygen.

PHOTOCHEMICAL FORMATION OF HYDROGEN AND OXYGEN

The decomposition of water into its elements

$$H_2O \longrightarrow H_2 + 1/2\ O_2$$

is endergonic by 56 kcal mol^{-1} at 25°C and may be considered in terms of the half-reactions for its reduction to hydrogen and oxidation to oxygen. These half-reactions are

$$e^- + H_2O = OH^- + 1/2\ H_2$$

$$1/2\ H_2O = H^+ + 1/4\ O_2 + e^-$$

The reduction potentials for these reactions are -0.41 and +0.82 V, respectively, at pH 7 with 1 atm pressure as the standard state for the gases. These potentials reflect the overall thermodynamic requirements for the half reactions, but since both involve multiequivalent changes the thermodynamics of the intermediate oxidation states of hydrogen and oxygen are also relevant. Some of these are presented in Table 5.

The reduction potentials for the ground and excited state couples of a number of the polypyridine complexes are summarized in Fig. 5. At the left-hand side, couples relevant to the reduction of water to H_2 are shown; their potentials may be compared with the pH-dependent potential for water reduction given by the straight line. Analogous data relevant to the oxidation of water to O_2 are displayed at the right-hand side of the figure. Couples with potentials below -0.82 V can produce H_2 at any pH $\lesssim$ 14, while those with potentials above 1.23 V are capable of producing oxygen at pH $\gtrsim$ 0. Couples with potentials between these limits can produce H_2 or O_2 under restricted pH conditions. It is evident that $^*Ru(bpy)_3^{2+}$ can reduce water to H_2 at pH $\lesssim$ 14 and oxidize water to O_2 at pH $\gtrsim$ 7. Similarly, $^*Cr(bpy)_3^{3+}$ can oxidize water to O_2 at pH $\gtrsim$ 0, but cannot reduce water in an accessible pH range. However no direct reduction or oxidation of water by these excited states has been reported.

TABLE 5. Reduction potentials relevant to the oxidation and reduction of water at 25°C and pH 7.0.[a]

Redox Couple	E^{o}(V)
$H^{+} + e^{-} = H$	-2.69
$H + e^{-} = H^{-}$	+0.03
$H^{+} + 2e^{-} = H^{-}$	-1.33
$OH + e^{-} = OH^{-}$	+2.33
$H_2O_2 + e^{-} = OH + OH^{-}$	+0.38
$H_2O_2 + 2e^{-} = 2OH^{-}$	+1.35
$2H^{+} + O_2^{-} + e^{-} = H_2O_2$	+0.82
$O_2 + e^{-} = O_2^{-}$	-0.28

[a] The standard state of H_2 and O_2 is 1 atmosphere pressure.

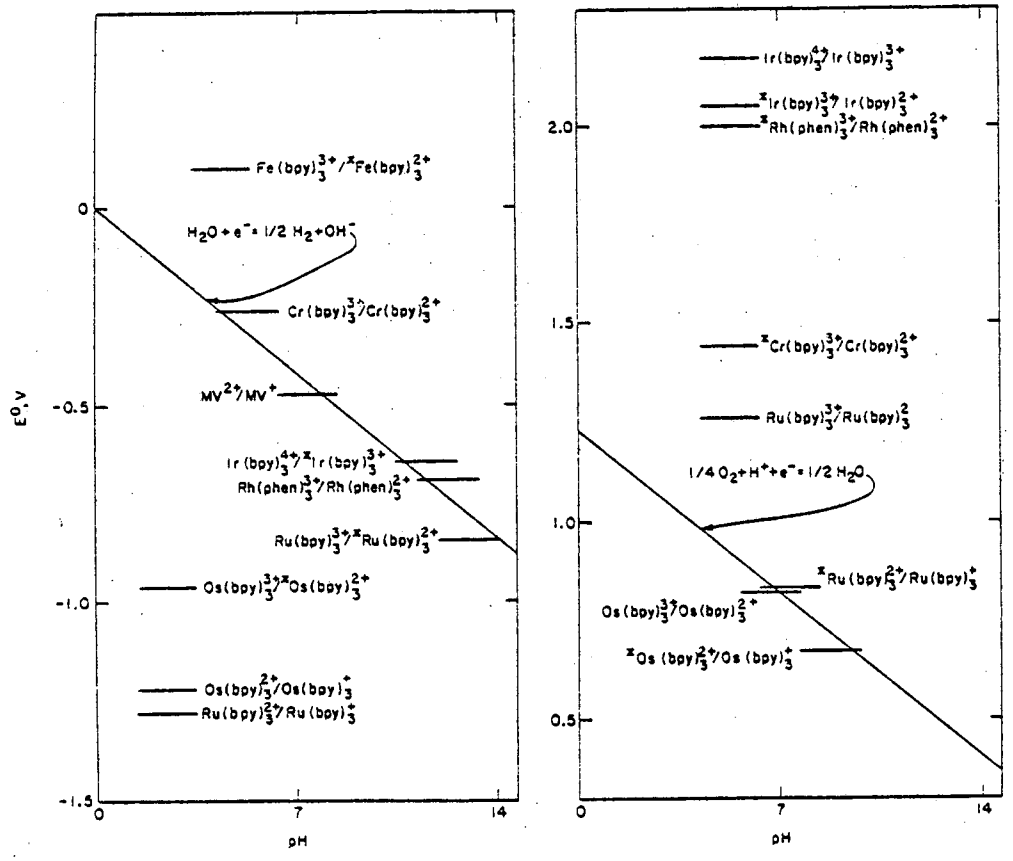

Fig. 5. Redox potentials for polypyridine couples relevant to water reduction (left-hand side) and water oxidation (right-hand side). The straight lines give the pH dependence of the water couples.

While it is apparent from Fig. 5 that a number of the couples are thermodynamically capable of effecting the overall reduction or oxidation of water, it is also clear that very few of the species are sufficiently strong reductants to carry out the one-electron reduction of water to hydrogen atoms or sufficiently powerful oxidants to produce free hydroxyl radicals. (By contrast, the ultraviolet sensitization of water decomposition by aquo-ions and other species does proceed by radical pathways (49).) Thus these complexes are not likely to mediate visible-light induced decomposition of water via one-electron transfer processes in the absence of catalysts capable of stabilizing the radical products. In addition, because of the relatively short lifetimes of the excited states and the rapidity of the back reactions, oxidation-reduction reactions involving additional solute species may be useful in producing hydrogen and/or oxygen. A general storage cycle involving light-induced electron transfer between a donor D and an acceptor A, and dark reactions of the oxidized donor D^+ with water or with the reducing agent Red, and of the reduced acceptor A^- with water or with the oxidant Ox, is presented in Scheme III.

Scheme III

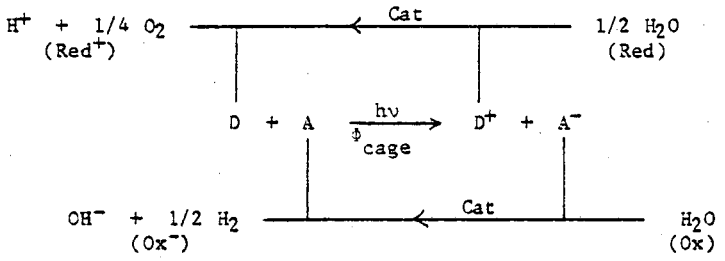

This scheme may involve either oxidative or reductive quenching of the excited state (i.e., either D = $^*M(bpy)_3^{n+}$ and A = Q, or D = Q and A = $^*M(bpy)_3^{n+}$). When both D^+ and A^- react with H_2O the overall cycle effects the photodecomposition of water into its elements. As mentioned above, the reactions of A^- and D^+ are expected to require catalysts if hydrogen and/or oxygen is to be evolved. No confirmed case of visible-light induced decomposition of water into both its elements has been reported. Therefore we now treat systems in which either hydrogen or oxygen has been produced from water.

Hydrogen formation reactions

Hydrogen evolution has been observed in a number of polypyridine-complex sensitized systems. Both oxidative and reductive quenching processes have been involved, several organic reducing agents have proven useful as either D or Red, and both heterogeneous and homogeneous catalysts (Cat) have been successful. Since hydrogen is produced, Ox is H_2O; because oxygen is not produced, Red or D is consumed. The systems for which quantum yield data have been reported are summarized in Table 6. The individual systems will be discussed in turn.

$Ru(bpy)_3^{2+}$, MV^{2+}, TEOA or EDTA. This system is the one that has been the most extensively studied in recent years. A reducing agent (Red) is added to scavenge the $Ru(bpy)_3^{3+}$ produced in the quenching reaction (eq 27,28). In the absence of a catalyst the MV^+ accumulates in the solution while in the presence of a catalyst it rapidly reacts with water

$$^*Ru(bpy)_3^{2+} + MV^{2+} \longrightarrow Ru(bpy)_3^{3+} + MV^+ \qquad (27)$$

$$Ru(bpy)_3^{3+} + Red \longrightarrow Ru(bpy)_3^{2+} + Red^+ \qquad (28)$$

$$2MV^+ + 2H_2O \xrightarrow{Cat} 2MV^{2+} + 2OH^- + H_2 \qquad (29)$$

to produce hydrogen (eq 29). Although a variety of reducing agents can be used (50), the best characterized systems are these where Red = triethanolamine (TEOA) (51-53) or EDTA (54-58). In the case of TEOA the optimum pH for hydrogen formation is ~ 7 and is determined by two opposing factors: the efficiency of hydrogen production by MV^+ drops with increasing pH as the water/hydrogen potential becomes more negative. On the other hand, the pK_a of TEOA is 8.1 and the unprotonated TEOA is the active reductant (51,27,28). The TEOA radical produced in the scavenging reaction (eq 28) rapidly abstracts (k = 0.3 x 107 M^{-1} s^{-1}) an H

TABLE 6. Summary of components and quantum yields for H_2-producing systems based on metal polypyridine complex sensitizers.

Donor	Acceptor	ϕ_{cage}	Red	Cat	pH	ϕ_{H_2}	Ref.
$^*Ru(bpy)_3^{2+}$	MV^{2+}	0.25	EDTA	Pt(PVA)	5	0.13	56
$^*Ru(bpy)_3^{2+}$	$Rh(bpy)_3^{3+}$	0.15	TEOA	Pt	7-8	0.11	29
$^*Ru(bpy)_3^{2+}$	$Rh(bpy)_3^{3+}$	0.15	EDTA	—	5	0.04	29
TEOA	$^*Rh(bpy)_2Cl_2^{+}$ [a]	—	—	—	8.5	0.02	64
Eu_{aq}^{2+}	$^*Ru(bpy)_3^{2+}$	1.0	—	$Co^{II}L$	1	0.05	65
ascorbate	$^*Ru(bpy)_3^{2+}$	~0.5	—	$Co^{II}L$	3.1	0.0005	65
TEA[b]	$^*Ru(bpy)_3^{2+}$	—	—	PtO_2	—	0.53	47
TEA[b]	$^*RuL_3^{2+}$ [c]	~0.4	—	PtO_2	—	0.44	47
EDTA	$^*CrL_3^{3+}$ [d]	—	—	Pt(PVA)	4.8	0.08	68

[a] Irradiation at 302 nm.
[b] The medium is acetonitrile containing 0.3 M TEA and 25% water.
[c] L is the di-isopropyl ester of 4,4'-dicarboxy-2,2'-bipyridine.
[d] L = 4,4'-$(CH_3)_2$bpy or 4,7-$(CH_3)_2$phen.

atom from another TEOA molecule to produce a very reducing radical (eq 30). The latter very rapidly reduces MV^{2+} ($k > 10^8$ M^{-1} s^{-1}) to produce a second MV^+ (eq 31). The theoretical quantum yield for MV^+ production in the TEOA system is thus 2.0 (note, however, that the maximum quantum yield for MV^+ formation is limited to ~ 0.50 by the cage escape yield of 0.25 (29)). The catalysts that have been used include colloidal Pt (54), hydrogenase (53),

$$TEOA^+ + TEOA \longrightarrow TEOAH^+ + TEOA' \quad (30)$$

$$TEOA' + MV^{2+} \longrightarrow (TEOA)^{2+} + MV^+ \quad (31)$$

and suspensions of PtO_2 (51). (It has been proposed that the catalytic action of the PtO_2 (Adams catalyst) arises from the formation of Pt at the surface of the PtO_2 (59).) Low yields of H_2 in the absence of an added catalyst have also been reported (52).

Most of the studies have been done with the reductant EDTA for which the optimum pH for hydrogen formation is ~ 5. There is some recent evidence that the EDTA radical produced in the scavenging reaction at pH 7 is converted into a reducing radical which yields a second MV^+ (58). These reactions are analogous to the TEOA reactions discussed above; as will be seen, triethylamine also undergoes a similar set of reactions. Hydrogen evolution rates in the $Ru(bpy)_3^{2+}$, MV^{2+}, EDTA system have been used as the standard for comparing the efficiencies of different catalysts, including colloidal Pt stabilized with poly(vinyl alcohol) (PVA) (56,59), and suspensions of PtO_2 and other metal oxides (59). In general, the colloidal systems are much more efficient than the metal oxide suspensions. Measurements of the effect of particle size and catalyst concentration in the Pt(PVA) system show that the rate of hydrogen evolution is increased sixfold upon decreasing the radii of the colloidal particles from 500 to 100 Å; for particles of 100 Å radius the hydrogen evolution rate is also increased sixfold upon increasing the Pt concentration from 8 mg L^{-1} to 120 mg L^{-1} (56). A quantum yield of 0.13 has been reported with the Pt(PVA) catalyst at pH 5 (56). This quantum yield is close to one half of the cage escape yield, consistent with the interpretation that the EDTA radical does not produce a second MV^+ at pH 5. Recent studies show that the long-term stability of the MV^{2+} system is limited by Pt-catalyzed hydrogenation of MV^{2+} (57); this problem can be avoided by use of a photoelectrochemical cell in which the H_2 is evolved at a remote Pt electrode (60).

Despite the numerous studies using hydrophobic $Ru(bpy)_3^{2+}$ and MV^{2+} derivatives in the presence of micelles (41-44), no quantum yield data have been reported for these systems. Nevertheless, important photosensitized reactions with these derivatives present in phospholipid vesicle walls have been carried out: these studies are relevant to the design of systems in which H_2 and O_2 might be generated on opposite sides of a membrane. Thus photosensitized reduction of MV^{2+} in the external aqueous phase occurs when $(bpy)_2Ru(bpy(CONHC_{16}H_{33})_2)^{2+}$ and dihexadecylviologen ($(C_{16})_2V^{2+}$) are incorporated into the wall of a vesicle that contains EDTA in its interior (61). In a related study,

$(bpy)_2Ru(bpy(CONHC_{12}H_{25})_2)^{2+}$ and didodecylviologen ($(C12)_2V^{2+}$) were incorporated in the

vesicle wall and the EDTA was replaced by triethylamine (TEA): this study was interpreted in terms of reductive quenching of the Ru complex by TEA (43, 44). Photosensitization with microemulsions has also been reported (62).

$Ru(bpy)_3^{2+}$, $Rh(bpy)_3^{2+}$, TEOA. Irradiation of this sytem at pH 7-8 in the absence of platinum yields rhodium(I) and free bpy; in the presence of platinum, H_2 and very little free bpy are produced. It was originally proposed (27) that the H_2 was generated in the platinum(0)-catalyzed reactions of rhodium(I). However recent studies (28,29) show that instead the H_2 is produced in the platinum(0)-catalyzed reactions of rhodium(II). The Pt(0) is either added as colloidal Pt(PVA) or generated *in situ* through photo-induced reduction of K_2PtCl_4 or K_2PtCl_6. The reactions occurring in this system are summarized in Fig. 6.

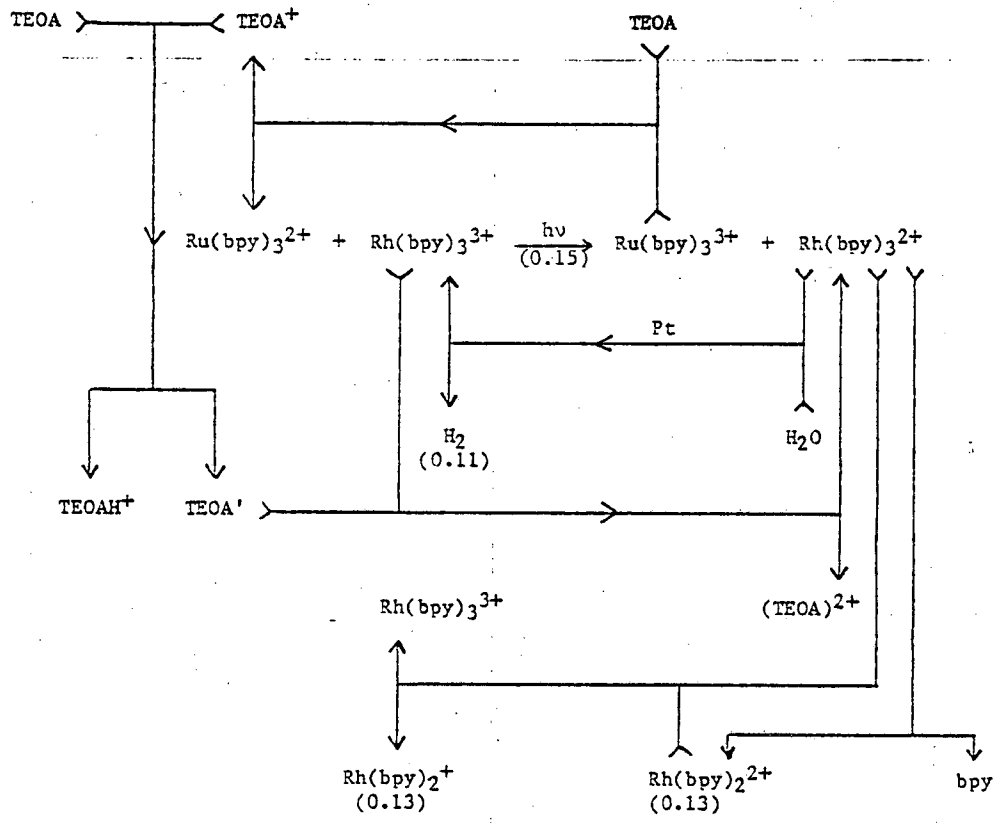

Fig. 6. Reaction pathways in the $Ru(bpy)_3^{2+}$ sensitized photoreduction of $Rh(bpy)_3^{3+}$ by TEOA in the presence and absence of platinum. The numbers in parentheses are quantum yields for the various processes.

The $^*Ru(bpy)_3^{2+}$ is oxidized by $Rh(bpy)_3^{3+}$ to produce $Ru(bpy)_3^{3+}$ and $Rh(bpy)_3^{2+}$. The $Ru(bpy)_3^{3+}$ is reduced by TEOA and the TEOA radical produced in this step, after undergoing a rearrangement (as discussed above for MV^{2+}), reduces $Rh(bpy)_3^{3+}$. In the absence of platinum the $Rh(bpy)_3^{2+}$ undergoes aquation and then oxidizes $Rh(bpy)_3^{2+}$ (disproportionates) as follows:

$$Rh(bpy)_2^{2+} + Rh(bpy)_3^{2+} \longrightarrow Rh(bpy)_2^{+} + Rh(bpy)_3^{3+} \qquad (32)$$

The rhodium(I) produced in eq 32 can exist in a variety of chemical forms, depending on the pH and rhodium(I) concentration of the solution (63). At very low concentrations the dominant forms of rhodium(I) at high and low pH are $Rh(bpy)_2^+$ and the hydride $Rh(bpy)_2(H_2O)H^{2+}$, respectively. At higher rhodium(I) concentrations the dimers $[Rh(bpy)_2]_2^{2+}$ and $[Rh(bpy)_2]H^{3+}$ predominate. None of these species produce significant quantities of H_2 over platinum; indeed the formation of hydrogen in these systems is not thermodynamically favorable. Experiments in which $Rh(bpy)_2(H_2O)_2^{3+}$ is added to the $Rh(bpy)_3^{3+}$ prior to the photolysis confirm that the H_2 is formed through the reactions of $Rh(bpy)_3^{2+}$ at platinum. Hardly any H_2 is produced in the presence of $Rh(bpy)_2(H_2O)_2^{3+}$. This can be explained as follows: the $Rh(bpy)_2(H_2O)_2^{3+}$ is reduced to $Rh(bpy)_2^{2+}$ which rapidly reacts with $Rh(bpy)_3^{2+}$ leading to the formation of rhodium(I) (eq 32). Because of

the rapid scavenging of $Rh(bpy)_3^{2+}$, very little hydrogen is produced in this sequence. The quantum yield for H_2 in the absence of added $Rh(bpy)_2(H_2O)_2^{3+}$ is 0.11, close to the cage escape yield of 0.15 and to the quantum yield of 0.13 for rhodium(I) and bpy formation in the absence of added platinum. Evidently the reactions converting the primary products are fairly efficient. Another interesting feature of this system is that it is capable of producing H_2 at pH 5 in the absence of platinum with EDTA as reductant (27,29). The quantum yield for H_2 formation under these conditions is 0.04.

As discussed earlier, $^*Rh(phen)_3^{3+}$ is a very powerful oxidant. In recent experiments it has been reduced to $Rh(phen)_3^{2+}$ with dimethylaniline (11). This observation is relevant to the report that photolysis of $Rh(bpy)_2Cl_2^+$ with ultraviolet light in the presence of TEOA at pH 8.5 produces H_2 with a quantum yield of 0.02 in the absence of added platinum (64). Like the platinum-free $Ru(bpy)_3^{2+}$ sensitized $Rh(bpy)_3^{3+}$ system at pH 5 (29), this ultraviolet photolysis features a long induction period. These induction periods may correspond to generation of homogeneous, catalytic rhodium species (possibly a rhodium(I) complex) which promote the reduction of water by the rhodium(II) generated by reaction of $Rh(bpy)_3^{3+}$ with $^*Ru(bpy)_3^{2+}$ or, in the $Rh(bpy)_2Cl_2^+$ system, by direct reduction of excited rhodium(III) by TEOA. (However, in the $Rh(bpy)_2Cl_2^+$ ultraviolet photolysis, H_2 could instead arise from photolysis of Rh(II) or from TEOA radical reactions rather than from thermal reactions of Rh(II).)

$Ru(bpy)_3^{2+}$, $Co(Me_6[14]diene\ N_4)(H_2O)_2^{2+}$, Eu_{aq}^{2+} or ascorbate. This system (65) is homogeneous and it has been proposed that the H_2 formation proceeds via $Ru(bpy)_3^+$ as follows:

$$^*Ru(bpy)_3^{2+} + D \longrightarrow Ru(bpy)_3^+ + D^+$$

$$Ru(bpy)_3^+ + Co^{II}L \longrightarrow Ru(bpy)_3^{2+} + Co^{I}L$$

$$Co^{I}L + H_3O^+ \longrightarrow Co^{III}L(H_2O)(H^-) \longrightarrow Co^{III}L(H_2O)_2 + H_2$$

$$Co^{III}L(H_2O)_2 + D \longrightarrow Co^{II}L + D^+$$

Here $Co^{II}L$ represents the cobalt macrocyclic complex. The quantum yields for H_2 formation are 0.05 and 5×10^{-4} when D = Eu_{aq}^{2+} and ascorbate, respectively. The above sequence possesses several interesting features. $Ru(bpy)_3^+$ rather than $^*Ru(bpy)_3^{2+}$ is used to reduce the cobalt complex: the reason for this is that the cobalt(II) complex is not reduced by the excited state. It may, however, be reduced by $Ru(bpy)_3^+$ since the latter has a longer lifetime and is a better reductant than $^*Ru(bpy)_3^{2+}$. No added platinum catalyst is required because the $Co^{I}L$ complex protonates at low pH to give an unstable Co^{III}hydride which rapidly reacts with acid to produce hydrogen and $Co^{III}L$. The relatively low quantum yields observed reflect the fact that the $Co^{I}L$ species is highly reactive and undergoes unproductive side reactions (e.g., reaction with ascorbate (65)).

The cobalt and the platinum-free rhodium systems at pH 7-8 possess several common features which are illustrated in Scheme IV. In each case the parent d^6 complex is reduced to a

Scheme IV

$$d^6 + e^- \longrightarrow d^7 \qquad (33)$$

$$d^7 + e^- \longrightarrow d^8 \qquad (34)$$

$$d^8 + H_3O^+ \longrightarrow d^6(H_2O)(H^-) \qquad (35)$$

coordinatively unsaturated d^8 complex which, in acidic solution undergoes oxidative addition of H_3O^+ to form a d^6 hydride (eq 35). The hydride in the cobalt system is very unstable and spontaneously decomposes to the parent d^6 complex and hydrogen. For thermodynamic reasons the hydride in the rhodium system does not yield H_2 even in the presence of platinum. Obviously the formation of a hydride is only fruitful from the standpoint of H_2 formation if the hydride formed is relatively unstable.

$Ru(bpy)_3^{2+}$ or $Ru(bpy(COOR))_3^{2+}$, TEA. $Ru(bpy)_3^{2+}$ and the hydrophobic ruthenium(II) complex $Ru(bpy(COOR))_3^{2+}$ where R is the isopropyl group are reductively quenched by triethylamine (TEA) in water-acetonitrile mixtures (46). The TEA radical produced in the quenching step rapidly reacts with TEA to form a very reducing radical (47) (compare the TEOA and EDTA radical reactions mentioned earlier). As a consequence RuL_3^+ accumulates in the solution and the theoretical quantum yield for RuL_3^+ formation is 2.0. Irradiation in the presence of PtO_2 yields H_2 with initial quantum yields of 0.53 and 0.44 for photolysis of $Ru(bpy)_3^{2+}$ and of $Ru(bpy(COOR))_3^{2+}$, respectively. The H_2 is presumably formed through PtO_2-catalyzed reactions of RuL_3^+, although catalyzed reactions of the secondary TEA radical with water have not been ruled out (47,48).

ML_3^{3+}-sensitized systems. Included in Table 6 are preliminary results for CrL_3^{3+}, EDTA systems (68). In these, $^*CrL_3^{3+}$ is reduced to CrL_3^{2+} which produces H_2 at the Pt catalyst. Although the initial quantum yield for H_2 formation is relatively high, the rate of H_2 evolution rapidly decreases because of the photoaquation of the chromium(III) complex. The use of polypyridine complexes of rhodium(III) and iridium(III) as sensitizers has also been reported to lead to H_2 formation (27).

$Rh_2(bridge)_4^{2+}$. We include here, for comparison purposes, some observations on binuclear rhodium complexes even though in this instance hydrogen production does not occur via $M(bpy)_3^{n+}$ sensitization. Photolysis of the binuclear complex $Rh_2(bridge)_4^{2+}$ (bridge = 1,3-diisocyanopropane) in concentrated HX (X = Cl, Br) produces H_2 and $Rh_2(bridge)_4X_2^{2+}$ (69,70). The formation of H_2 in this system proceeds both thermally and photochemically according to the following reactions:

$$2[Rh^{I}(bridge)_4Rh^{I}]^{2+} + 2HCl \longrightarrow [Rh^{I}(bridge)_4Rh^{II}Cl]_2^{4+} + H_2$$

$$[Rh^{I}(bridge)_4Rh^{II}Cl]_2^{4+} + 2HCl \xrightarrow{h\nu} 2[ClRh^{II}(bridge)_4Rh^{II}Cl]^{2+} + H_2$$

In 1 N H_2SO_4 the binuclear rhodium(I) complex can be oxidized to the mixed-valence dimer $[Rh^{I}(bridge)_4Rh^{II}]_2^{6+}$ which produces H_2 and $[Rh^{II}(bridge)Rh^{II}]^{4+}$ upon photolysis. It has been proposed (71) that this reaction may proceed via two parallel paths, one producing a mixed-valence complex (eq 36) and the other yielding binuclear rhodium(II) and rhodium(I) complexes (eq 37). Thermal reaction of the rhodium(I) dimer produces hydrogen and the mixed-valence dimer (eq 38).

$$[Rh^{I}(bridge)_4Rh^{II}]_2^{6+} \xrightarrow{h\nu} 2[Rh^{I}(bridge)_4Rh^{II}]^{3+} \quad (36)$$

$$\xrightarrow{h\nu} [Rh^{II}(bridge)_4Rh^{II}]^{4+} + [Rh^{I}(bridge)_4Rh^{I}]^{2+} \quad (37)$$

$$2[Rh^{I}(bridge)_4Rh^{I}]^{2+} + 2H^{+} \longrightarrow [Rh^{I}(bridge)_4Rh^{II}]_2^{6+} + H_2 \quad (38)$$

Photoproduction of hydrogen is not cyclic in this system, but rather occurs at the expense of $Rh_2(bridge)_4^{2+}$.

General Comments. In each of the systems in Table 6 the net reaction is eq 39,

$$(Red \text{ or } 2\,Red) + 2H^{+} \xrightarrow{h\nu} (Red^{2+} \text{ or } 2\,Red^{+}) + H_2 \quad (39a)$$

$$(D \text{ or } 2D) + 2H^{+} \xrightarrow{h\nu} (D^{2+} \text{ or } 2D^{+}) + H_2 \quad (39b)$$

that is, the hydrogen is produced at the expense of an added electron donor. When this donor is an amine, subsequent reactions of the primary radical convert it to a powerful reducing agent (27,47,51,66). A possible mechanism for these reactions is shown in Scheme V where the R-substituted amine (R = $-CH_2CH_2OH$ for TEOA, etc.) is symbolized as R_2NCH_2R'.

Scheme V

$$R_2\ddot{N}CH_2R' \longrightarrow R_2\dot{\overset{+}{N}}CH_2R' + e^{-}$$

$$R_2\dot{\overset{+}{N}}CH_2R' + R_2\ddot{N}CH_2R' \longrightarrow [R_2\overset{H}{\overset{+}{N}}CH_2R']^{+} + R_2\ddot{N}-\dot{C}HR'$$

$$[R_2\ddot{N}-\dot{C}HR' \longleftrightarrow R_2\dot{N}{=}CHR'] \longrightarrow R_2\overset{+}{N}{=}CHR' + e^{-}$$

$$R_2\overset{+}{N}{=}CHR' + H_2O \longrightarrow R_2NH + R'CHO + H^{+}$$

Although the second reaction has been written as a hydrogen abstraction, it could involve proton transfer. In any event, as a consequence of the production of the reducing radical, two reducing equivalents are produced per photon absorbed and the theoretical quantum yield for H_2 formation in the amine-based systems is therefore 1.0. Despite the fact that the primary radical produced in the ascorbate system does not undergo a similar set of reactions, it is rapidly converted to a non-oxidizing radical through a disproportionation reaction (34,35,67). The theoretical quantum yield for H_2 formation in ascorbate-based systems is thus 0.5. The fact that the primary radicals are rapidly converted to non-oxidizing species is what makes the organic reductants so useful in these systems.

It is apparent from Table 6 that the highest quantum yield is obtained with the Et_3N system and the lowest with the $Co^{II}L$, ascorbate system. In both, $Ru(bpy)_3^{+}$ is formed as an intermediate in relatively high yield. In the Et_3N system the $Ru(bpy)_3^{+}$ (or $Et\dot{\overset{+}{N}}{=}CHCH_3$) reacts directly at the PtO_2 catalyst to produce hydrogen, a process which is evidently very

efficient. In the $Co^{II}L$, ascorbate system, the $Ru(bpy)_3^{+}$ is used to reduce $Co^{II}L$ to a hydride which does not produce hydrogen efficiently under the homogeneous conditions used. The other $Ru(bpy)_3^{2+}$-sensitized systems in Table 6 involve the formation of $Rh(bpy)_3^{2+}$ or MV^{+}, both of which produce hydrogen efficiently on the platinum catalyst used.

While a fair battery of heterogeneous catalysts for hydrogen formation now exists, few such resources have been developed in the area of homogeneous catalysis. The homogeneous catalysts are likely to be species capable of binding hydrogen atoms or hydride ions with binding constants that are not too large. Historically, efforts have been focussed on the problems of hydrogen dissociation (activation of hydrogen as a reducing agent), that is, on the reverse of the reactions required in the photodecomposition of water. Metal complexes as diverse as $Co(CN)_5^{3-}$, Cu_{aq}^{2+}, Ag_{aq}^{+}, chloro-aquo complexes of Ru(III) and Rh(III), and d^8 complexes of Rh(I) and Ir(I) promote the dissociation of hydrogen (89). Microscopic reversibility arguments and observations on these catalysts indicate that hydrogen formation might be accomplished by the following kinds of processes, depending on the nature of the catalyst M.

Heterolytic combination:

$$M^{III}(H^{-}) + H^{+} \longrightarrow M^{III} + H_2$$

Homolytic combination:

$$2\ M^{II}H \longrightarrow 2\ M^{II} + H_2$$

Reductive elimination:

$$M^{III}(H^{-})_2 \longrightarrow M^{I} + H_2$$

The metal hydride intermediates, $M^{III}H^{-}$, $M^{II}H$, or $M^{III}(H^{-})_2$, would derive either from A^{-} in Scheme III or from reduction of M^{III} or M^{II} by the reduced acceptor. Unfortunately, with the exception of the cobalt macrocycle and the $Rh_2(bridge)_4^{2+}$ species discussed earlier, all the metal complexes known to bring about the dissociation or the formation of hydrogen in aqueous solution do so only very slowly. Slow hydrogen formation reactions are not tolerable in most systems since the precursors (A^{-}), being very strong reducing agents, rapidly undergo side reactions. In view of the stringent demands on the homogeneous catalyst, it is not surprising that heterogeneous catalysts have been the more widely used.

Oxygen formation reactions

Photochemical formation of oxygen has been accomplished using the $Ru(bpy)_3^{2+}$, $Co(NH_3)_5Cl^{2+}$ system (eq 40-42). Quenching of $^{*}Ru(bpy)_3^{2+}$ by $Co(NH_3)_5Cl^{2+}$ (D and A, respectively, in Scheme III) gives $Ru(bpy)_3^{3+}$ in very high yield (72,73). Rapid, irreversible aquation of $Co(NH_3)_5Cl^{+}$ produces the poor reductant Co_{aq}^{2+}. The reaction of $Ru(bpy)_3^{3+}$ (D^{+}) with H_2O (Red) in the presence of colloidal or suspended catalysts produces oxygen.

$$^{*}Ru(bpy)_3^{2+} + Co(NH_3)_5Cl^{2+} \longrightarrow Ru(bpy)_3^{3+} + Co(NH_3)_5Cl^{+} \qquad (40)$$

$$Co(NH_3)_5Cl^{+} + 5\ H^{+} \longrightarrow Co_{aq}^{2+} + 5\ NH_4^{+} + Cl^{-} \qquad (41)$$

$$Ru(bpy)_3^{3+} + 1/2\ H_2O \xrightarrow{Cat} Ru(bpy)_3^{2+} + H^{+} + 1/4\ O_2 \qquad (42)$$

Catalysts that have been used at pH 1-4 include RuO_2 suspensions (74,75), and iridium or ruthenium oxides deposited on alumina (74) or zeolites (76). A photoelectrochemical cell (using $Co(C_2O_4)_3^{3-}$ as the acceptor) in which the oxygen is generated at a remote platinum electrode has also been described (82). In other studies at pH 6-8 in the absence of metal oxides, evidence was obtained that the hydrolyzed cobalt(II) formed in eq 41 may itself act as an oxygen formation catalyst (77). The rate of oxygen formation was at a maximum in a pH 7 phosphate buffer, the quantum yield being 0.02-0.03. Although the system is translucent initially, a precipitate of cobalt hydroxide rapidly develops during the early stages of the photolysis.

The "reduction" of $M(bpy)_3^{3+}$ (M = Fe, Ru, or Os) to $M(bpy)_3^{2+}$ in alkaline solution has been recognized for many years (78-80) and oxygen has been identified as a product for $Fe(bpy)_3^{3+}$ and $Ru(bpy)_3^{3+}$. The reaction of $Ru(bpy)_3^{3+}$ with water and hydroxide ion has been extensively studied and observations made on this system illustrate the complexities likely to be found in homogeneous oxygen formation reactions. The rate of $Ru(bpy)_3^{2+}$ production is first order in $Ru(bpy)_3^{3+}$ at low (< 5) and very high (> 12) pH and the rate law contains terms zero-, first-, and second-order in hydroxide ion (80). Oxygen was, however, a major product only between pH 8 and 10, a region in which the kinetics were extremely complicated. Nucleophilic addition of H_2O or OH^{-} to the bpy ring in $Ru(bpy)_3^{3+}$ was postulated as the rate-determining step in the reaction and the variation of oxygen yield with pH was ascribed

to pH and ruthenium(III)-dependent reactions of $Ru(bpy)_3OH^{2+}$ adducts (80). More recently it was proposed that oxygen is a product of $Ru(bpy)_3^{3+}$ reduction only in the presence of hydroxo iron(III) or other transition metal ions (77). Reinvestigation has indicated that the solutions used in the original studies may have contained micromolar amounts of iron(III) and that much smaller O_2 yields are indeed obtained in the absence of iron(III) or other trace metals (81).

The catalysis of water oxidation by transition metal ions and oxides has stimulated much research in the past few years (59,76,83,84). Higher yields of oxygen from water are obtained with $IrCl_6^{2-}$ and $M(bpy)_3^{3+}$ (M = Fe, Ru,) as oxidants when hydroxo cobalt(II) species are present (77). In addition to cobalt(II) and iron(III), hydroxo complexes of iron(II), nickel(II), and copper(II) are also effective catalysts for oxygen formation in alkaline solutions of $Ru(bpy)_3^{3+}$ (77). Oxidation of the hydroxo complexes by $Ru(bpy)_3^{3+}$ has been invoked and the high oxidation states, i.e. Co(IV), Fe(IV), Ni(IV), etc., have been postulated to oxidize water in a two-electron transfer process, e.g. for iron the -yl state (ferryl, FeO^{2+}) which may generate peroxide either upon reaction with H_2O or OH^-, eq 43, or in a bimolecular reaction, eq 44. The peroxide is then oxidized to oxygen.

$$FeO^{2+} + OH^- \longrightarrow Fe^{2+} + HO_2^- \qquad (43)$$

$$2\ FeO^{2+} + H_2O \longrightarrow FeOH^{2+} + Fe^{3+} + HO_2^- \qquad (44)$$

It has not yet been established whether the active catalysts are in fact homogeneous since the hydroxo ions may be highly polymerized and consequently colloidal under the conditions used. In the $Ru(bpy)_3^{3+}$ system an alternative mechanism should also be considered: the hydroxo complexes may serve to divert the $Ru(bpy)_3OH^{2+}$ adducts so that water (rather than ligand) oxidation is the dominant net reaction.

Future directions

We have seen that the photoreduction of water to hydrogen using bipyridine complexes and visible light has been accomplished with reasonably high efficiency in a number of systems. Efforts to carry out the analogous photooxidation of water to oxygen have met with less success, but recent reports are encouraging. It is now established that the relatively strong reducing (e.g. $Ru(bpy)_3^{+}$) and oxidizing (e.g. $Ru(bpy)_3^{3+}$) intermediates required for these processes may be generated in high yields. While the direct reduction and oxidation of water by these intermediates appears to be very slow in the absence of catalysts, there has been a steady improvement in the efficiencies of the heterogeneous catalysts so that only relatively low concentrations are now required (59,74-76,83,84). Models in which the heterogeneous catalysts are treated as micro-electrodes have been developed: for example, the use of RuO_2 suspensions to promote water oxidation by $Ru(bpy)_3^{3+}$ was suggested by the low overvoltage for water oxidation at an RuO_2 electrode (59,84). Similarly, the ability of Pt suspensions to promote hydrogen evolution could be related to the low overvoltage for water reduction at a platinum electrode. In most cases the heterogeneous catalysts have been separately prepared and then added to the photolysis system; however in some instances the catalysts have been prepared *in situ*, for example, by the reduction of $PtCl_4^{2-}$ (27-29) or Ag^+ (85). Finely divided metals prepared in this manner are highly reactive (86) and are finding application in a variety of processes (86-88).

While the photoproduction of hydrogen *or* oxygen from water has been the subject of most studies, the ultimate goal of work in this area is *simultaneous* formation of hydrogen and oxygen. Efforts to attain this goal have so far met with little success: recently photolysis of $Ru(bpy)_3^{2+}$, MV^{2+} solutions containing RuO_2 (to promote the oxidation of water by $Ru(bpy)_3^{3+}$) *and* colloidal Pt (to catalyze the reduction of water by MV^+) was reported to produce hydrogen and oxygen simultaneously (75). Although this is an encouraging result, a recent attempt to reproduce the findings failed (58). The simultaneous generation of hydrogen and oxygen requires the use of highly specific catalysts in order to avoid the short-circuiting of the cycle through the cross-reaction of the reduced and oxidized intermediates. The latter intermediates are also very reactive toward oxygen and hydrogen, respectively, so that the gaseous products must be rapidly removed from solution. These problems can be largely avoided if the oxidation and reduction processes are carried out in different spatial regions, separated, for example, by a membrane. In fact, studies with RuL_3^{2+} and MV^{2+} have already demonstrated the feasibility of separating donor and acceptor sites by the use of vesicles (43,44,61). In view of these considerations, substantial progress in this area is likely to derive only from a judicious blend of well-designed catalysts, compartments, and chemistry.

Acknowledgment - This paper was presented at the VIIIth IUPAC Symposium on Photochemistry, held at Seefeld, Austria, 13-19 July 1980. The work was performed under contract with the U. S. Department of Energy and supported by its Office of Basic Energy Sciences.

REFERENCES

1. N. Sutin and C. Creutz, Adv. Chem. Ser. No. 168, 1-27 (1978).
2. N. Sutin, J. Photochem. 10, 19-40 (1979).
3. V. Balzani, F. Bolletta, M. T. Gandolfi and M. Maestri, Top. Curr. Chem. 75, 1-64 (1978).
4. V. Balzani, F. Bolletta, F. Scandola and R. Ballardini, Pure and Appl. Chem. 51, 299-311 (1979).
5. M. Maestri, F. Bolletta, L. Moggi, V. Balzani, M. S. Henry and M. Z. Hoffman, J. Am. Chem. Soc. 100, 2694-2701 (1978).
6. B. Brunschwig and N. Sutin, J. Am. Chem. Soc. 100, 7568-7577 (1978).
7. C. Creutz, M. Chou, T. L. Netzel, M. Okumura and N. Sutin, J. Am. Chem. Soc. 102, 1309-1319 (1980).
8. B. T. Ahn and D. R. McMillin, Inorg. Chem. 16, 943-945 (1977); 17, 2253-2258 (1978). G. Ferraudi, Inorg. Chem. 17, 1370-1372 (1978).
9. J. N. Demas, E. W. Harris and R. P. McBride, J. Am. Chem. Soc. 99, 3547-3551 (1977); C. M. Flynn, Jr. and J. D. Demas, J. Am. Chem. Soc. 96, 1959-1960 (1974).
10. J. N. Demas, E. W. Harris, C. M. Flynn, Jr. and D. Diemente, J. Am. Chem. Soc. 97, 3838-3839 (1975).
11. R. Ballardini, G. Varani and V. Balzani, J. Am. Chem. Soc. 102, 1719-1720 (1980).
12. D. G. Taylor and J. N. Demas, J. Chem. Phys. 7, 1032-1033 (1979); F. Bolletta, A. Juris, M. Maestri and D. Sandrini, Inorg. Chim. Acta 44, L175-176 (1980).
13. J. Van Houten and R. J. Watts, Inorg. Chem. 17, 1381-1385 (1978).
14. N. A. P. Kane-Maguire, J. Conway and C. H. Langford, J. Chem. Soc., Chem. Comm. 801-802 (1974).
15. G. A. Crosby, W. G. Perkins and D. M. Klassen, J. Chem. Phys. 43, 1498-1503 (1965).
16. J. N. Demas and G. A. Crosby, J. Am. Chem. Soc. 93, 2841-2847 (1971).
17. G. A. Crosby and W. H. Elfing, Jr., J. Phys. Chem. 80, 2206-2211 (1976).
18. E. L. Wehry and S. Sundarajan, J. Chem. Soc., Chem. Comm. 1135 (1972); S. Sundarajan and E. L. Wehry, J. Phys. Chem. 76, 1528-1536 (1972).
19. A. B. P. Lever, Inorganic Electronic Spectroscopy, Elsevier, London (1968).
20. J. K. Yandell and M. A. Augustin, Inorg. Chem. 18, 577-583 (1979).
21. N. Sutin, Acc. Chem. Res. 1, 225-231 (1968).
22. B. S. Brunschwig, J. Logan, M. D. Newton and N. Sutin, J. Am. Chem. Soc. 102, in press; M. Chou, C. Creutz and N. Sutin, J. Am. Chem. Soc. 99, 5615-5623 (1977).
23. R. A. Marcus, J. Chem. Phys. 43, 679-701 (1965).
24. N. S. Hush, Trans. Farad. Soc. 57, 557-580 (1961).
25. J. Ulstrup and J. Jortner, J. Chem. Phys. 63, 4358-4368 (1975).
26. J. V. Beitz and J. R. Miller, J. Chem. Phys. 71, 4579-4595 (1979), and references cited therein.
27. M. Kirch, J.-M. Lehn and J. P. Sauvage, Helv. Chim. Acta 62, 1345-1384 (1979).
28. G. M. Brown, S.-F. Chan, C. Creutz, H. A. Schwarz and N. Sutin, J. Am. Chem. Soc. 101, 7638-7640 (1979).
29. S.-F. Chan, M. Chou, C. Creutz, T. Matsubara and N. Sutin, J. Am. Chem. Soc., submitted.
30. A. P. Zipp, to be published.
31. R. Ballardini, G. Varani, F. Scandola and V. Balzani, J. Am. Chem. Soc. 98, 7432-7433 (1976).
32. C.-T. Lin, W. Böttcher, M. Chou, C. Creutz and N. Sutin, J. Am. Chem. Soc. 98, 6536-6544 (1976).
33. C. Creutz, Inorg. Chem. 17, 1046-1051 (1978); C. Creutz and N. Sutin, J. Am. Chem. Soc. 98, 6384-6386 (1976).
34. C. Creutz, N. Sutin and B. S. Brunschwig, J. Am. Chem. Soc. 101, 1297-1298 (1979).
35. E. Pelizetti, E. Mentasti and E. Pramauro, Inorg. Chem. 15, 2898-2900 (1976).
36. C.-T. Lin, M. A. Hoselton, H. A. Schwarz and N. Sutin, J. Am. Chem. Soc. 100, 2383-2388 (1978).
37. A. Haim and N. Sutin, Inorg. Chem. 15, 476-478 (1976).
38. R. A. Marcus and N. Sutin, Inorg. Chem. 14, 213-216 (1975).
39. D. Meisel, M. S. Matheson and J. Rabani, J. Am. Chem. Soc. 100, 117-122 (1978).
40. E. Pelizetti and E. Pramauro, Inorg. Chem. 19, 882-883 (1979).
41. P.-A. Brugger and M. Grätzel, J. Am. Chem. Soc. 102, 2461-2463 (1980).
42. Y. Tsutsui, K. Takuma, T. Nishijima and T. Matsuo, Chem. Lett. 617-620 (1979).
43. T. Matsuo, K. Takuma, Y. Tsutsui and T. Nishijima, J. Coord. Chem. in press.
44. T. Matsuo, T. Nagamura, K. Itoh and T. Nishijima, Memoirs Faculty Eng. Kyushu Univ. 40, 25-36 (1980).
45. M. Grätzel, Isr. J. Chem. 18, 364-368 (1979).
46. P. J. DeLaive, J. T. Lee, H. Abruna, H. W. Sprintschnik, T. J. Meyer and D. G. Whitten, Adv. Chem. Ser. No. 168, 28-43 (1978).
47. P. J. DeLaive, B. P. Sullivan, T. J. Meyer and D. G. Whitten, J. Am. Chem. Soc. 101, 4007-4008 (1979).
48. D. G. Whitten, Acc. Chem. Res. 13, 83-90 (1980).
49. G. Stein and A. Zeichner, Solar Energy 23, 11-16 (1979).
50. A. I. Krasna, Photochem. and Photobiol. 31, 75-82 (1980).

51. K. Kalyanasundaram, J. Kiwi and M. Grätzel, Helv. Chim. Acta 61, 2720-2730 (1978).
52. M. Gohn and N. Getoff, Z. Naturforsch. 34a, 1135-1139 (1979).
53. I. Okura and N. Kim-Thuan, J. Mol. Cat. 5, 311-314 (1979).
54. A. Moradpour, E. Amouyal, P. Keller and H. Kagan, Nouv. J. Chim. 2, 547-549 (1978).
55. J. Kiwi and M. Grätzel, Nature 281, 657-658 (1979).
56. J. Kiwi and M. Grätzel, J. Am. Chem. Soc. 101, 7214-7217 (1979).
57. P. Keller, A. Moradpour, E. Amouyal and H. Kagan, J. Mol. Cat. 7, 539-542 (1980).
58. P. Keller, A. Moradpour, E. Amouyal and H. B. Kagan, Nouv. J. Chim. in press.
59. J. Kiwi, Isr. J. Chem. 18, 369-374 (1979).
60. B. Durham, W. Dressick and T. J. Meyer, J. Chem. Soc., Chem. Comm. 381 (1979).
61. W. E. Ford, J. W. Otvos and M. Calvin, Nature 274, 507-508 (1978).
62. I. Willner, W. E. Ford, J. W. Otvos and M. Calvin, Nature 280, 823-824 (1979).
63. A. P. Zipp, M. Chou, C. Creutz and N. Sutin, work in progress.
64. K. Kalyanasundaram, Nouv. J. Chim. 3, 511-515 (1979).
65. G. M. Brown, B. S. Brunschwig, C. Creutz, J. F. Endicott and N. Sutin, J. Am. Chem. Soc. 101, 1298-1300 (1979).
66. P. J. Smith and C. K. Mann, J. Org. Chem. 34, 1821-1826 (1969).
67. B. H. J. Bielski, D. A. Comstock and R. A. Bowen, J. Am. Chem. Soc. 93, 5624-5629 (1971).
68. R. Ballardini, A. Juris, G. Varani and V. Balzani, submitted for publication.
69. V. M. Miskowski, I. S. Sigal, K. R. Mann, H. B. Gray, S. J. Milder, G. S. Hammond and P. R. Ryason, J. Am. Chem. Soc. 101, 4383-4385 (1979).
70. H. B. Gray, K. R. Mann, N. S. Lewis, J. A. Thich and R. M. Richman, Adv. Chem. Ser. No. 168, 44-56 (1978).
71. K. R. Mann, M. J. DiPierro and T. P. Gill, J. Am. Chem. Soc. 102, 3965-3967 (1980). K. R. Mann, I. S. Sigal and H. B. Gray, submitted for publication.
72. H. D. Gafney and A. W. Adamson, J. Am. Chem. Soc. 94, 8238-8239 (1972).
73. G. Navon and N. Sutin, Inorg. Chem. 13, 2159-2164 (1974).
74. J.-M. Lehn, J.-P. Sauvage and R. Ziessel, Nouv. J. Chim. 3, 423-427 (1980).
75. K. Kalyanasundaram and M. Gratzel, Angew. Chem. Int. Ed. Engl. 18, 701-702 (1979).
76. J.-M. Lehn, J. P. Sauvage and R. Ziessel, Nouv. J. Chim. in press.
77. V. Ya. Shafirovich, N. K. Khannov and V. V. Strelets, Nouv. J. Chim. 4, 81-84 (1980).
78. M. Anbar and I. Pecht, Trans. Farad. Soc. 64, 744-750 (1968), and references cited therein.
79. G. Nord and O. Wernberg, J. Chem. Soc., Dalton Trans. 845-849 (1975).
80. C. Creutz and N. Sutin, Proc. Nat. Acad. Sci. USA 72, 2858-2862 (1975).
81. M. Chou and N. Sutin, work in progress.
82. D. P. Rillema, W. J. Dressick and T. J. Meyer, J. Chem. Soc., Chem. Comm. 247-248 (1980).
83. J. Kiwi and M. Grätzel, Angew. Chem. Int. Ed. Engl. 17, 860-861 (1978).
84. J. Kiwi and M. Grätzel, Chimia 33, 289-291 (1979).
85. T. K. Foreman, C. Giannotti and D. G. Whitten, J. Am. Chem. Soc. 102, 1170-1171 (1980).
86. R. D. Rieke, Acc. Chem. Res. 10, 301-306 (1977).
87. A. Henglein, Angew. Chem. Int. Ed. Engl. 18, 418 (1979).
88. C. K. Grätzel and M. Grätzel, J. Am. Chem. Soc. 101, 7741-7743 (1979).
89. J. Halpern, Ann. Rev. Phys. Chem. 16, 103-121 (1965).